microorganisms

MDPI

Article

Microbiome Skincare Innovation: Unsupervised Segmentation for Targeted Formulations

Hye-Been Kim [1,2], Uyen Thy Nguyen [3], MyeongHyun Yoou [3], Nikita Lukianets [3], Elsa Jungman [3], HyungWoo Jo [1], Minji Kim [1], Misun Kim [1], Dong-Geol Lee [1], Chun Ho Park [1], Yunsuk Nam [4], Sangho Lee [4], James Joo [4], Dong Keon Yon [2,5], Seunghyun Kang [6,*] and Haryung Grace Park [3,*]

[1] COSMAX BTI, InnoValley E, 255, Pangyo-ro, Bundang-gu, Seongnam-si 13486, Gyeonggi-do, Republic of Korea
[2] Department of Precision Medicine, Kyung Hee University, Seoul 02447, Republic of Korea
[3] HelloBiome, ELSI Skin Health Inc., 181 2nd St, San Francisco, CA 94105, USA; thy@hellobio.me
[4] COSMAX USA, 105 Challenger Rd, Ridgefield Park, New Jersey, NJ 07660, USA; james.joo@cosmax.com
[5] Department of Pediatrics, Kyung Hee University Medical Center, Kyung Hee University, Seoul 02447, Republic of Korea
[6] COSMAX, InnoValley E, 255, Pangyo-ro, Bundang-gu, Seongnam-si 13486, Gyeonggi-do, Republic of Korea
* Correspondence: shyunk@cosmax.com (S.K.); grace@hellobio.me (H.G.P.)

Abstract

The skin microbiome plays a crucial role in skin health, yet most skincare products are developed without accounting for interindividual microbiome variation. To address this limitation, we aimed to develop and validate a microbiome-informed skincare formulation. Using unsupervised machine learning (*k*-means clustering) applied to 23 microbiome-derived features—diversity indices, bacterial and fungal relative abundances, and a compound microbiome score—from 862 participants, we identified eight skin segments with distinct microbial signatures and clinical characteristics. The largest segment (n = 364) was selected to guide formulation development, and the resulting skincare regimen was evaluated in an independent clinical cohort recruited based on the skin phenotype associated with this segment. For this segment, we developed a cleanser and serum containing postbiotic ferments and evaluated the ingredients in vitro and the complete skincare regimen in a 6-week clinical study. In UV-exposed human dermal fibroblasts, *Streptococcus* ferment Fillerstin increased *COL1A1* expression and reduced *MMP-1* expression, while *Corynebacterium* ferment Ambioter suppressed *IL-1β* expression; both ingredients showed no evidence of irritation or sensitization under the tested conditions. Furthermore, use of the complete skincare regimen containing postbiotic ferments was associated with improvements in skin hydration, sebum levels, elasticity, skin texture, evenness, and luminosity. No statistically significant changes in skin microbiome alpha or beta diversity were detected during the study, and correlations between clinical severity and the associated species weakened after serum application. These findings provide preliminary support for microbiome-informed skincare formulation development, although controlled clinical studies are needed to establish ingredient-specific efficacy and the clinical benefits of personalization.

Keywords: skin microbiome; personalized skincare; postbiotic ferment; precision cosmetics

Academic Editor: Rafael Bargiela

Received: 19 September 2026
Revised: 19 November 2026
Accepted: 19 November 2026
Published: 24 November 2026

Copyright: © 2026 by the authors. Licensee MDPI, Basel, Switzerland. This article is an open access article distributed under the terms and conditions of the Creative Commons Attribution (CC BY) license.

1. Introduction

The human skin, with an estimated epithelial surface area of at least 30 m^2 when hair follicles and other skin appendages are included, serves as a dynamic habitat for a complex microbial community comprising bacteria, fungi, viruses, and microeukaryotes—collectively termed the skin microbiome [1–4]. This ecosystem exhibits a unique composition distinct from other body sites such as the gut, oral cavity, and vaginal microbiome, largely due to the skin's challenging environmental conditions [1,2,5], including selective nutrient availability, acidic pH from 4.5 to 5.5, low temperature (29–34 °C), variable moisture levels, sebum composition, and host immunological factors. Core bacterial genera include *Staphylococcus*, *Corynebacterium*, and *Cutibacterium*, alongside fungal genus *Malassezia*. These core microbial communities vary across skin sites, with sebaceous areas harboring lipophilic organisms while moist regions support diverse microbial profiles [6,7]. Community composition and function are highly responsive to both external environmental influences—such as temperature, humidity, and cosmetic use—and intrinsic host factors, including skin barrier conditions and inflammation [8,9].

Culture-based studies have illuminated critical roles of these key microbial members, including antimicrobial defense through competitive exclusion of pathogens [10–12], modulation of immune responses [13–15], and maintenance of skin barrier integrity [16,17]. The advent of next-generation, high-throughput DNA sequencing technologies has revolutionized our understanding of microbiome complexity, enabling cultivation-independent profiling of entire communities rather than only culturable organisms [18–20]. While these advanced methods have successfully distinguished microbial signatures associated with various dermatological conditions including diabetic wounds [21–23], atopic dermatitis [24], psoriasis [25], and acne vulgaris [26,27], comprehensive characterization of the healthy skin microbiome across diverse populations and age groups remains surprisingly underexplored. This knowledge gap presents a significant opportunity to establish baseline parameters for normal skin microbial communities, which could inform therapeutic and innovative approaches targeting specific skin segmentation based on the microbiome.

The bidirectional relationship between the skin and its microbiota means that microbial communities not only shape skin health but also serve as measurable biomarkers of dermatological conditions. Alterations in skin microbial diversity and community composition have been associated with various dermatological conditions, including acne and inflammatory skin disorders, as well as skin aging [24–29]. Thus, profiling the skin microbiome provides a potential analytical framework for developing individualized dermatological regimens that align with an individual's biological and microbial profile [30,31]. However, these references describe industry-oriented research and applications rather than peer-reviewed clinical validation. Personalization helps target the unique immunological and physiological needs of each skin type, improving efficacy while minimizing irritation or imbalance [32,33].

In recent years, increasing attention has been directed toward harnessing the microbiome in skincare innovation. Active compounds derived from beneficial microbes—often termed postbiotics—are now being integrated into cosmetic formulations. These microbiome-derived ingredients can help rebalance dysbiotic skin, reinforce epidermal defenses, and promote immune tolerance, while avoiding the drawbacks of broad-spectrum antimicrobials [34]. Importantly, such formulations can be tailored based on microbiome composition of specific skin types or conditions, offering the potential for more effective and personalized skincare solutions.

Previous studies have demonstrated the potential of skin-derived *Streptococcus* species and their secreted metabolites to improve skin structure and barrier function [35].

https://doi.org/10.3390/microorganisms14122742

Furthermore, a topical postbiotic formulation derived from *S. pneumoniae*, *S. mitis*, and *S. infantis* demonstrated clinical efficacy in patients with mild-to-moderate atopic dermatitis [36]. Subsequent analyses of the same clinical trial identified differences in treatment responses according to the presence of allergic comorbidities [37]. In addition, a recent preprint reported the skin-related biological activities of culture filtrates derived from *Corynebacterium amycolatum* SB-1, including effects on skin-associated gene expression and melanogenesis [38]. Collectively, these findings provide a scientific rationale for investigating microbial fermentation-derived ingredients in microbiome-informed skincare formulations.

To achieve this, we employed an unsupervised machine learning approach using microbial features, which generated eight distinct clusters. From these, we focused on the largest cluster to demonstrate how skin microbiome data can be leveraged in the development of personalized skincare products. By aligning skincare formulations with specific microbial and physiological profiles, we aim to enhance the precision, relevance, and efficacy of microbiome-based cosmetic solutions.

2. Materials and Methods

2.1. Participant and Recruitment Criteria for Study Population

For clustering analysis, the study included participants who completed a skin microbiome kit (n = 862) on our platform. This general cohort comprised self-selected direct-to-consumer users and participants from previous platform studies, without demographic or eligibility restrictions based on age, sex, ethnicity, geography, or skin condition. Each completed kit with a valid microbiome profile was included. Therefore, the cohort was not restricted to adults, and its representativeness of a defined population could not be established. Privacy Policy was followed throughout participant information processing. All analyses were performed using deidentified data. Distinct clusters of skin microbial profiles were identified through unsupervised machine learning techniques (k-means clustering). The analysis included 23 microbiome-derived variables comprising four diversity and summary indices, the relative abundances of 12 bacterial species and six fungal taxa, and a compound microbiome score. The sequencing provider reported absolute abundance values only for detected microorganisms. These values were converted to relative abundances, and absent taxon entries were assigned a value of zero to represent non-detection rather than missing measurements. This procedure ensured a consistent set of microbial features across samples. All features were subsequently Z-score standardized. k-means clustering was performed using k-means + + initialization, 1000 restarts, a fixed random seed, and Euclidean distance. Candidate cluster numbers (k = 3–17) were evaluated using the elbow method and silhouette score. The final solution used k = 10, which provided the most favorable cluster separation and evaluation scores among the candidate solutions. The two smallest clusters (n = 1 and n = 2) were assigned to an unclassified group because their extremely small sample sizes made them potentially sensitive to noise, resulting in eight retained clusters (Table S3). Among the eight identified clusters, Cluster 1 (n = 364) was selected for further analysis based on its large sample size, its characteristic microbial composition associated with oily or combination skin and inflammation-related concerns, and the feasibility of developing a targeted postbiotic formulation and recruiting a phenotypically matched clinical cohort.

Fifty-five female participants with diverse ethnic backgrounds within the US between ages 20–45 were recruited in an independent cohort. Participants were eligible if they had mild to moderate fine lines (approximately 50% of the study population), uneven skin tone, oily or combination skin, rough skin texture, vascular dark circles (approximately 50% of the study population), visible pores, and self-perceived regular breakouts (minimum once per month or more) or mild to moderate acne. Exclusion

criteria included pregnancy, breastfeeding, or menopause; eczema or psoriasis on the forehead; systemic, autoimmune, or immunodeficiency disorders; medical procedures on the face within the last year; known allergies to skin treatment products or cosmetics; a history of skin cancer; and diabetics. A total of 55 female participants aged 20–45 years were enrolled in the clinical study. Of these, 43 participants completed the six-week study, while 12 discontinued participations (11 were lost to follow-up and one withdrew for personal reasons). Among the 43 completers, one participant was excluded from the longitudinal microbiome analysis due to a missing baseline microbiome sample, resulting in a final microbiome analysis cohort of 42 participants, while clinical assessments included all 43 completers. The demographic and self-reported characteristics of these 42 participants are summarized in Table 1. HelloBiome's privacy policy was strictly followed for participant information processing collected through the HelloBiome platform and kits. All analyses were performed on de-identified data.

Table 1. Demographic distribution of study participants enrolled in clinical study for postbiotic treatment.

Age Group *	**20s (20–29 Years)**	**30s (30–39 Years)**	**40s (40–45 Years)**	**Total ******
	***n* = 12**	***n* = 22**	***n* = 8**	***n* = 42**
Ethnicity				
American Indian or Alaska Native	1 (8.3%)	0 (0.0%)	0 (0.0%)	1 (2.4%)
Asian	1 (8.3%)	2 (9.1%)	0 (0.0%)	3 (7.1%)
Black or African American	2 (16.7%)	3 (13.6%)	5 (62.5%)	10 (23.8%)
Hispanic or of Spanish origin, Latinx	4 (33.3%)	7 (31.8%)	0 (0.0%)	11 (26.2%)
Multiple	3 (25.0%)	1 (4.5%)	1 (12.5%)	5 (11.9%)
White or Caucasian	1 (8.3%)	9 (40.9%)	2 (25.0%)	12 (28.6%)
Skin Type				
Don't Know **	0 (0.0%)	1 (4.5%)	0 (0.0%)	1 (2.4%)
Balanced	0 (0.0%)	0 (0.0%)	1 (12.5%)	1 (2.4%)
Combination	9 (75.0%)	17 (77.3%)	6 (75.0%)	32 (76.2%)
Dry	1 (8.3%)	2 (9.1%)	0 (0.0%)	3 (7.1%)
Oily	2 (16.7%)	2 (9.1%)	1 (12.5%)	5 (11.9%)
Fitzpatrick Skin Phototype ***				
Fitzpatrick Skin Phototype I	0 (0.0%)	2 (9.1%)	0 (0.0%)	2 (4.8%)
Fitzpatrick Skin Phototype II	1 (8.3%)	3 (13.6%)	1 (12.5%)	5 (11.9%)
Fitzpatrick Skin Phototype III	5 (41.7%)	7 (31.8%)	2 (25.0%)	14 (33.3%)
Fitzpatrick Skin Phototype IV	1 (8.3%)	6 (27.3%)	2 (25.0%)	9 (21.4%)
Fitzpatrick Skin Phototype V	5 (41.7%)	3 (13.6%)	3 (37.5%)	11 (26.2%)
Fitzpatrick Skin Phototype VI	0 (0.0%)	1 (4.5%)	0 (0.0%)	1 (2.4%)
Hormonal Breakouts				
Don't Know	0 (0.0%)	3 (13.6%)	2 (25.0%)	5 (11.9%)
No	3 (25.0%)	1 (4.5%)	1 (12.5%)	5 (11.9%)
Yes	9 (75.0%)	18 (81.8%)	5 (62.5%)	32 (76.2%)
Hormonal Changes				
Peri-menopausal	0 (0.0%)	1 (4.5%)	1 (12.5%)	2 (4.8%)
Pre-menopausal	12 (100.0%)	21 (95.5%)	7 (87.5%)	40 (95.2%)
Facial Skin Concerns				
None	2 (16.7%)	1 (4.5%)	1 (12.5%)	4 (9.5%)
Acne/breakouts	5 (41.7%)	10 (45.5%)	4 (50.0%)	19 (45.2%)
Hyperpigmentation	0 (0.0%)	0 (0.0%)	1 (12.5%)	1 (2.4%)
Multiple	5 (41.7%)	10 (45.5%)	2 (25.0%)	17 (40.5%)
Rosacea	0 (0.0%)	1 (4.5%)	0 (0.0%)	1 (2.4%)

Recurring Skin Concerns				
None	0 (0.0%)	4 (18.2%)	0 (0.0%)	4 (9.5%)
Acne/Breakouts	10 (83.3%)	12 (54.5%)	5 (62.5%)	27 (64.3%)
Dryness	1 (8.3%)	2 (9.1%)	1 (12.5%)	4 (9.5%)
Oiliness	1 (8.3%)	4 (18.2%)	2 (25.0%)	7 (16.7%)
Skin Sensitivity				
No	3 (25.0%)	10 (45.5%)	4 (50.0%)	17 (40.5%)
Yes	9 (75.0%)	12 (54.5%)	4 (50.0%)	25 (59.5%)
Sensitivity-Related Concerns				
None	9 (75.0%)	8 (36.4%)	3 (37.5%)	20 (47.6%)
Itching	0 (0.0%)	1 (4.5%)	0 (0.0%)	1 (2.4%)
Multiple	0 (0.0%)	6 (27.3%)	3 (37.5%)	9 (21.4%)
Redness	1 (8.3%)	2 (9.1%)	2 (25.0%)	5 (11.9%)
Sensations of heat	0 (0.0%)	3 (13.6%)	0 (0.0%)	3 (7.1%)
Skin irritability	1 (8.3%)	1 (4.5%)	0 (0.0%)	2 (4.8%)
Tautness (tight)	1 (8.3%)	1 (4.5%)	0 (0.0%)	2 (4.8%)

* Age groups were defined as 20–29, 30–39, and 40–45 years based on the eligibility criteria of the clinical study, which enrolled female participants aged 20–45 years. ** Note: "Don't know" indicates that participants were uncertain about their response, whereas "None" indicates that no applicable condition or concern was reported. *** Skin phototypes were classified according to the Fitzpatrick skin phototype scale (Types I–VI). **** Values are presented as *n* (%). Percentages were calculated based on the number of respondents in each group.

2.2. Self-Report Metrics Protocol

Participants were given a standardized questionnaire each time a swab sample was collected to gather self-reported information regarding (1) demographic characteristics such as gender, ethnicity, location, and age; (2) lifestyle factors such as diet, facial routines, and product usage habits, and skincare goals; (3) skin types (e.g., oily, dry, combination); and (4) current skin issues (e.g., acne, dryness, hormonal breakouts). All responses were collected through the HelloBiome platform.

2.3. Product Usage Protocol

The study took place over 6 weeks. Participants used a facial cleanser containing postbiotic ferments twice daily (morning and evening) for 2 weeks as an addition to their regular skincare routine. For the subsequent 4 weeks, participants replaced their routine entirely with the cleanser and serum, used twice daily. Product ingredients for the cleanser and serum are listed in Tables 2 and 3, respectively.

Table 2. Formulation Ingredient List of Cleanser.

No *	Name
010	Water
020	Acrylates/C10-30 Alkyl Acrylate Crosspolymer
030	Glycerin
040	Diglycerin
050	Panthenol
060	Hydroxyacetophenone
070	Water, Lauryl Hydroxysultaine, Sodium Chloride
080	Water, Sodium Methyl Cocoyl Taurate
090	Water, Sodium Cocoyl Alaninate
100	Water, Cocamidopropyl Betaine, Sodium Chloride, Sodium Benzoate

110	Xylitylglucoside, Anhydroxylitol, Water, Xylitol
120	Water, Sodium Cocoyl Apple Amino Acids, Hexylene Glycol, Tetrasodium Glutamate Diacetate
130	Water, Sodium Lauroyl Oat Amino Acids
140	Water, Polyquaternium-7, Sodium Benzoate
150	Caprylyl Glycol
160	Ethylhexylglycerin, Tocopherol
170	Water
180	Tromethamine
190	Water, Butylene Glycol, Corynebacterium Ferment, 1,2-Hexanediol
200	Water, Butylene Glycol, Streptococcus Pneumoniae Ferment Extract Filtrate, Streptococcus Mitis Ferment Extract Filtrate, Streptococcus Infantis Ferment Extract Filtrate, 1,2-Hexanediol
210	Allantoin
220	Water, 1,2-Hexanediol, Sodium Hyaluronate Crosspolymer, Butylene Glycol, Xylose, Polyglutamic Acid, Ethylhexylglycerin
230	Butylene Glycol, Water, Fomes Officinalis (Mushroom) Extract
240	Tetrahexyldecyl Ascorbate
250	Sorbitol, Water
260	Saccharomyces Ferment Filtrate, Sodium Benzoate, Potassium Sorbate
270	Tocopherol
280	Niacinamide

* Note: "No." indicates the ingredient identification number used to describe the formulation procedure in Section 2.10.

Table 3. Formulation Ingredient List of Serum.

No *	Name
010	Water
020	Panthenol
030	Sodium Phytate
040	Sorbitol, Water
050	Niacinamide
060	Allantoin
070	Acacia Senegal Gum, Xanthan Gum
080	Glycerin, Methylpropanediol
090	Polyacrylate Crosspolymer-6
100	Polyglyceryl-3 Distearate, Glyceryl Stearate Citrate
110	Glyceryl Stearate
120	Squalane
130	Caprylic/Capric Triglyceride
140	Ethylhexylglycerin, Tocopherol
150	Phenoxyethanol
160	Saccharomyces Ferment Filtrate, Sodium Benzoate, Potassium Sorbate
170	Water, 1,2-Hexanediol, Butylene Glycol, Corynebacterium Ferment
180	Water, 1,2-Hexanediol, Butylene Glycol, Streptococcus pneumoniae Ferment Extract Filtrate, Streptococcus mitis Ferment Extract Filtrate, Streptococcus infantis Ferment Extract Filtrate
190	Water, 1,2-Hexanediol, Sodium Hyaluronate Crosspolymer, Butylene Glycol, Xylose, Polyglutamic Acid
200	Tetrahexyldecyl Ascorbate
210	Tocopherol

220	Butylene Glycol, Water, Fomes Officinalis (Mushroom) Extract
230	Water, Salix Alba (Willow) Bark Extract

* Note: "No." indicates the ingredient identification number used to describe the formulation procedure in Section 2.10.

2.4. Skin Microbiome Sampling Protocol

Each sampling kit included sterile cotton swabs, buffer packs, detailed instructions, and return labels and boxes. For clustering analysis, participants followed a 24-h wash-out period prior to sample collection, avoiding any facial products or water. Microbiome swabs were self-collected from a quarter-sized region on the forehead between the eyebrows for 80 s, then stored in tubes containing DNA/RNA shield buffer at room temperature and shipped within 4 days of collection.

During the clinical study, microbiome samples were at three timepoints: at the start of the study (Baseline), after use of the facial cleanser (Week 2), and after usage of both cleanser and postbiotic serum (Week 6). Prior to each collection, participants followed a 24-h wash-out period, avoiding any facial products or water. Swabs were collected and stored using the protocol described above.

2.5. Microbiome Sequencing and Analysis

Microbial samples were collected with swabs and collection tubes prefilled with DNA/RNA Shield (R1100, Zymo Research, Irvine, CA, USA). DNA was extracted using ZymoBIOMICS-96 Magbead DNA Kit (D4302, Zymo Research, Irvine, CA, USA) with KingFisher System (Thermo Fisher Scientific, Waltham, MA, USA). Bacterial 16S ribosomal RNA (rRNA) V1–V3 and fungal Internal Transcribed Spacer 2 (ITS2) regions were sequenced using Quick-16S NGS Library Prep Kit (D6400, Zymo Research, Irvine, CA, USA) with automation performed with Hamilton STAR (Hamilton Company, Reno, NV, USA). Sequencing was performed by a third-party CLIA-CAP certified diagnostic lab. PCR reactions during the library preparation were performed on CFX384 Real Time PCR system (Bio-Rad Laboratories, Hercules, CA, USA) according to the instruction manual. PCR amplification was performed with the following cycling conditions: initial denaturation at 95 °C for 10 min; 42 cycles for 95 °C for 30 s, 55 °C for 30 s of annealing, and 72 °C for 3 min of extension; followed by a hold at 4 °C. The PCR products were quantified with RT-PCR Ct value before pooling. The PCR products (16s and ITS) were pooled in a 1:0.5 ratio. The final pooled library was cleaned using a customized kit from Zymo Research (Irvine, CA, USA), then the final pooled PCR product was quantified using Qubit. The NGS library was sequenced on the Illumina MiniSeq with the MiniSeq Mid Output Kit 300 cycles (Illumina, San Diego, CA, USA). The primer sequences used for 16S rRNA V1–V3 and fungal ITS2 amplification, excluding Nextera adapters (Illumina, San Diego, CA, USA), are provided in Supplementary Table S1. Positive and negative controls using cell and DNA mock communities were included as part of the NGS workflow. The DADA2 pipeline (v1.36.0) was used to remove potential sequencing errors and chimeric sequences [39]. The Femto Bacterial and Fungal DNA Quantification kits (Zymo Research Corporation, Irvine, CA, USA) were used to quantify absolute abundance of total bacteria and fungi according to the manufacturer's protocol [40]. A real-time PCR approach was utilized with primers targeting V1–V3 and ITS regions for bacterial and fungal quantification.

Raw reads were analyzed with DADA2 (v1.36.0) [39] to determine the true amplicon sequence variants (ASVs). Potential sequencing errors, chimeric sequences, and contaminants were removed using the DADA2 pipeline and a proprietary algorithm, respectively. The ASV taxonomy classifications were predicted based on search results from UCLUST [41] from Qiime (v.1.9.1) against a custom 16S and ITS database.

Optimization of the 16S and ITS databases was performed using GreenGene database [42] and UNITE database [43], respectively. Species-level identification using a related targeted sequencing approach was previously evaluated against shotgun sequencing in canine skin and ear samples [44].

R (v4.3.3; R Foundation for Statistical Computing, Vienna, Austria) and RStudio (Posit, Boston, MA, USA) with packages including phyloseq (v1.46.0) [45], MicroViz (v0.12.6), and ggplot2 (v3.5.1) were used to analyze and visualize microbiome load, diversity, and taxonomic composition in conjunction with the associated metadata. Pairwise comparisons were performed using Wilcoxon signed-rank test and Kruskal–Wallis test for multiple group comparisons, with adjustments using Benjamini–Hochberg correction for multiple comparisons.

2.6. Microbial Isolation and Culture

To develop skin-beneficial microbiome ingredients, *Streptococcus pneumoniae* BF00257 (KCCM12005P), *Streptococcus mitis* BF00251 (KCCM12656P), *Streptococcus infantis* BF00247 (KCCM12642P), and *Corynebacterium amycolatum* SB-1 (KCCM12689P) were isolated from facial skin samples. Facial skin microbiota samples were collected by washing the participants' faces with sterile distilled water, and the collected samples were spread onto Tryptic Soy Agar (TSA) plates for bacterial isolation [35,38]. The bacterial isolates were identified by 16S rRNA gene sequencing using the universal primers 27F and 1492R (Cosmogene Tech, Republic of Korea). The resulting sequences were analyzed using the NCBI BLASTN program for taxonomic identification. The strain identities and corresponding culture collection accession numbers are provided above. No additional isolation screening was performed in the present study. Instead, these four previously isolated strains were selected based on reported skin-related biological activities of their culture-derived preparation [35–38].

The isolated bacteria strains were stored at the COSMAX Microbiome Bank (CMB, COSMAXBTI Inc., Seongnam, Republic of Korea) and deposited at the Korean Culture Center of Microorganisms (KCCM, Seoul, Republic of Korea). A single colony of each bacterial strain was picked from an agar plate, inoculated into skin-mimetic broth (SMB), and incubated at 30 °C with shaking at 160 rpm for 48 h in the dark. After incubation, each culture was filtered using a syringe filter (0.45 μm pore size; Minisart, Sartorius, Germany). All culture filtrates were prepared in triplicate [46].

The cosmetic ingredients Fillerstin and Ambioter were manufactured by GFC Life Science (Gyeonggi-do, Republic of Korea). During manufacturing, the fermentation-derived preparations underwent centrifugation followed by filtration through a 0.22 μm membrane to remove bacterial cells. The manufactured ingredients were subjected to lot-specific quality control according to the manufacturer's specifications, including appearance, odor, pH, specific gravity, refractive index, heavy metals, and microbiological testing. Microbiological acceptance criteria included total viable aerobic counts (≤00 CFU/g), yeasts and moulds (≤100 CFU/g), and the absence of specified pathogens.

2.7. Cell Culture and Treatment

The human dermal fibroblast cell line Hs68 was obtained from the American Type Culture Collection (ATCC, Manassas, VA, USA). Hs68 cells were seeded at a density of 3.5×10^5 in a 6-well plate and cultured in Dulbecco's modified Eagle's medium (DMEM, Gibco, USA) supplemented with 1% antibiotic antimycotic (HyClone Laboratories, Logan, UT, USA) and 10% fetal bovine serum (FBS; HyClone Laboratories, Logan, UT, USA) for 24 h in an incubator at 37 °C and 5% CO_2. Immortalized human keratinocytes (HaCaT)

were also obtained from the ATCC. The cells were cultured in DMEM media supplemented with 10% FBS and incubated for 24 h in an incubator at 37 °C and 5% CO_2.

2.8. Gene Expression Analysis

The fermentation-derived components of Fillerstin and Ambioter were evaluated in the in vitro experiments. The bacterial cultures were grown to approximately 1×10^8 CFU/mL before filtration. The *Streptococcus* culture filtrate used for Fillerstin was derived from *Streptococcus pneumoniae*, *Streptococcus mitis*, and *Streptococcus infantis*, whereas the *Corynebacterium* culture filtrate used for Ambioter was derived from *Corynebacterium amycolatum*. Both culture filtrates were tested at 1% (*w*/*w*) without the additional preservative components present in the corresponding cosmetic ingredients. The complete cosmetic ingredients, Fillerstin and Ambioter, which contain the respective culture filtrates and preservative components, were used for ingredient-level safety assessments.

Primer sequences used for microbiome profiling and gene expression analysis are summarized in Table S1.

2.8.1. Barrier Enhancement Effect

For collagen type I alpha 1 chain (*COL1A1*) and matrix metalloproteinase-1 (*MMP-1*) assay in UV-irradiated condition, the Hs68's medium was removed, Dulbecco's phosphate-buffered saline (DPBS; Gibco, Grand Island, NY, USA) was added, and the cells were irradiated with or without 12 mJ/cm^2 of UVB (wavelength 290–320 nm, maximum peak 311 nm). After UVB irradiation, DPBS was removed and replaced with FBS-free DMEM media. *Streptococcus* culture filtrate [1% (*w*/*w*)] was treated and further incubated for 24 h. A sample treated with UV light, but no treatment was used as the negative control [47]. The gene expression of *COL1A1* and *MMP-1* was analyzed using qPCR.

2.8.2. Anti-Inflammation Effect

HaCaT cells were cultured in DMEM media supplemented with 10% FBS and incubated for 24 h in an incubator at 37 °C and 5% CO_2. The medium was changed every 3–4 days, and the cells were sub-cultured when they overgrew. Cells were seeded at a density of 5×10^5 cells/well and washed with phosphate-buffered saline (PBS) after 24 h of incubation. The cell medium was replaced with FBS-free DMEM, and 10 μg/mL polyinosinic–polycytidylic acid (Poly (I:C)) and 10 ng/mL interleukin 4 (IL-4) were added to induce inflammation [48]. *Corynebacterium amycolatum* culture filtrate [1% (*w*/*w*)] was added to the cells and incubated for 4 h. The gene expression of interleukin-1β (*IL-1β*) was analyzed using qPCR with the aforementioned conditions, except that the primers for *IL-1β* were used.

2.9. RNA Isolation and Real-Time PCR

Total RNA was isolated from cells using TRIzol reagent according to the manufacturer's instructions (TaKaRa, Shiga, Japan). cDNA was synthesized from 1 μg of total RNA using Reverse Transcription Premix (Elpis-biotech, Daejeon, Republic of Korea) under the following reaction conditions: cDNA synthesis at 45 °C for 45 min and heat inactivation at 95 °C for 5 min. Gene expression signals were quantified with real-time PCR, and the data were analyzed using StepOnePlus™ system software (v2.3; Applied Biosystems, Foster City, CA, USA). Real-time PCR amplification reactions were performed using SYBR Green PCR Master Mix with premixed ROX (Applied Biosys-tems, Foster City, CA, USA). The following primer pairs (Bioneer, Daejeon, Republic of Korea) were used in the reactions performed in an ABI 7300 following the manufacturer's

instructions. The reaction conditions were as follows: initiation at 50 °C for 2 min and 95 °C for 10 min, followed by cycling at 95 °C for 10 s and 60 °C for 1 min for 40 cycles. β-actin was used as an internal control.

2.10. Formulation

The cleanser was prepared by sequentially combining ingredients according to (Table 2). Ingredients [010, 020] were mixed in the main vessel at 250 rpm for 15 min, followed by the addition of Ingredient [030, 040, 050, 060] under agitation at 300 rpm and heated to 60–65 °C. Ingredients [070–110] were added with continuous mixing at 400 rpm and mixed for 15 min. After mixing, the batch was cooled to 40 °C, and ingredients [120, 130] were added sequentially. After mixing at 300 rpm for 3 min, ingredients [140–230] were added and mixed at 300 rpm for 5 min, followed by cooling to 30 °C to complete the formulation.

The serum was prepared by sequentially combining ingredients according to (Table 3). Ingredients [010–060] were mixed in the main vessel at 250 rpm for 5 min, followed by the addition of a premix of [070–080] under agitation at 300 rpm for 5 min. Ingredient [090] was then slowly added with continuous mixing at 500 rpm for 15 min. The mixture was heated to 75–80 °C. Separately, the oil phase ([100–130]) was prepared at 80 °C and gradually added to the main vessel. Emulsification was performed using a homogenizer (Primix, Tokyo, Japan) at 5000 rpm for 5 min. After emulsification, the batch was cooled to 40 °C, and ingredients [140–230] were added sequentially. A second homogenization was conducted at 5000 rpm for 3 min, followed by cooling to 30 °C to complete the formulation.

2.11. Safety Assessments

The safety of Fillerstin and Ambioter was evaluated using a bacterial reverse mutation test (Ames test), an in vitro skin irritation test, an in vitro eye irritation test, and a human repeat insult patch test (HRIPT). The three in vitro safety tests were conducted by Biotoxtech (Cheongju, Republic of Korea) in accordance with OECD Test Guidelines (TG) 471, 439, and 492, respectively. These studies were conducted in compliance with Good Laboratory Practice (GLP) standards, as documented in the final study reports.

The bacterial reverse mutation test (OECD TG 471) was performed using four *Salmonella typhimurium* strains (TA98, TA100, TA1535, and TA1537) and one *Escherichia coli* strain (WP2uvrA), with and without metabolic activation (S9 mix). Both ingredients were tested at concentrations ranging from 6.25% to 100% in the main assays. Skin irritation was evaluated according to OECD TG 439 using reconstructed human epidermis (KeraSkin™ tissues), with cell viability assessed by the MTT assay. Eye irritation was evaluated according to OECD TG 492 using reconstructed human cornea-like epithelium (MCTT HCE™ tissues), with cell viability assessed using WST-1.

HRIPTs were conducted using Fillerstin and Ambioter by P&K Skin Research Center (Seoul, Republic of Korea) in accordance with its standard operating procedures. A volume of 20 μL of each ingredient was applied to the back using an IQ Ultimate chamber (Chemotechnique Diagnostics, Vellinge, Sweden) secured with 3M Micropore Tape (3M, St. Paul, MN, USA). During the induction phase, nine patch applications were performed over three weeks, with each patch maintained for 24 h. Skin reactions were visually assessed approximately 1 h after patch removal. Following a two-week rest period without treatment, a 24 h challenge patch was applied to a previously untreated skin site. Skin responses were evaluated at 24 and 48 h after patch removal using modified Frosch–Kligman and CTFA criteria.

The final facial serum was separately evaluated for dermal irritation and sensitization potential in an HRIPT conducted by Eurofins CRL Cosmetics, LLC (Piscataway, NJ, USA),

according to study protocol CL 1.0 2022. The serum was tested as received under semi-occlusive patch conditions.

2.12. Statistical Analysis for In Vitro Cell Assay

Statistical analysis for all experiments was conducted using three independent biological replicates ($n = 3$), with each replicate independently performed from cell culture through experimental analysis. The results are presented as mean ± standard deviation. For in vitro cell assay analysis, statistical analysis was performed using the SPSS statistical package version 25.0 (SPSS Inc., Chicago, IL, USA). Statistical analyses were conducted with a two-tailed Student's t-test, and unadjusted p-values of less than 0.05 and 0.01 were considered statistically significant.

2.13. Skin Physiology Measurements

The left or right cheekbone used for instrumental measurements was randomized according to a computer-generated randomization schedule. Participants were blinded to the names of the test materials, whereas the investigatory staff was not blinded. Expert clinical grading was performed by a clinical research coordinator using predefined 0–9 scoring scales. Product application compliance was monitored through daily diaries reviewed by the clinical staff. Measurements included corneometer, cutometer, vapometer, sebumeter, and expert clinical grading. The corneometer assessed skin hydration via capacitance changes. The cutometer evaluated skin elasticity and viscoelasticity through vacuum suction (500 mm Hg), with five parameters recorded: R0 (firmness), R2 (gross elasticity), R5 (elasticity after deformation), R6 (viscoelastic-to-elastic ratio), and R7 (net elasticity).

Transepidermal water loss (TEWL) was assessed using a VapoMeter (Delfin Technologies, Kuopio, Finland). The instrument measures the increase in relative humidity within a closed measurement chamber and automatically calculates the evaporation rate, expressed in g/m²/h. Two measurements were obtained from the randomized cheekbone at each time point. The sebumeter quantified skin sebum content (μg/cm²) via translucency of a plastic strip after 30 s of skin contact. Clinical grading by the research coordinator assessed fine lines, skin tone evenness, skin texture, luminosity/radiance, vascular dark circles, and pore visibility on a 0–9 scale, with higher scores indicating greater severity.

Skin physiological parameters were measured using a Corneometer (Courage & Khazaka, Cologne, Germany), a Cutometer Dual MPA 580 equipped with a 2 mm probe (Courage & Khazaka, Cologne, Germany), a VapoMeter (Delfin Technologies, Kuopio, Finland), and a Sebumeter SM 815 (Courage & Khazaka, Cologne, Germany). Facial images were obtained using the VISIA-CR imaging system (Canfield Scientific, Parsippany, NJ, USA; CR-5).

Before each assessment, participants were acclimatized to ambient laboratory conditions for approximately 15 ± 5 min. Measurements were performed on the randomized left or right cheekbone. Three Corneometer measurements, two VapoMeter measurements, and two Sebumeter measurements were obtained at each assessment. Cutometer measurements were performed using a suction pressure of 500 mmHg, with three consecutive 20 s suction–relaxation cycles. The evaluated Cutometer parameters were R0, R2, R5, R6, and R7.

3. Results

3.1. Metadata and Microbiome Results of Cluster 1

In our investigation, we identified eight optimal skin microbiome clusters using unsupervised machine learning based on facial microbiome profiles. Among these, we focus on the largest cluster, Cluster 1 (n = 364), representing a substantial segment of the population. This cluster exhibits low microbial diversity, driven by the high dominance of lipophilic species *Cutibacterium acnes* and *Malassezia restricta* (Figure 1). Individuals within the cluster were subclustered into three groups: Healthy, those with no self-reported inflammatory skin conditions (e.g., acne, rosacea, eczema, or psoriasis); Inflamed, those who reported having such conditions; and Other*, those whose skin concerns were not clearly specified (Table 4).

Demographic analysis revealed distinctive characteristics among the subgroups of Cluster 1. Most individuals were in their 20s and 30s, with the Inflamed group showing a higher representation of younger participants (19–30 years old) in their early reproductive stage. Skin sensitivity patterns demonstrated clear group differentiation, with 64% of participants in the Healthy cohort reporting non-sensitive skin. Conversely, the Inflamed and Other groups reported skin sensitivity prevalence (66.9% and 64.7%, respectively). Further, Inflamed group exhibited higher proportions of combination and oily skin types relative to the Healthy group, while the Other group demonstrated the highest prevalence of dry skin type. Contrastingly, the Healthy cohort showed the highest percentage of balanced skin (39.5%), followed by combination-to-dry skin types (Table 4).

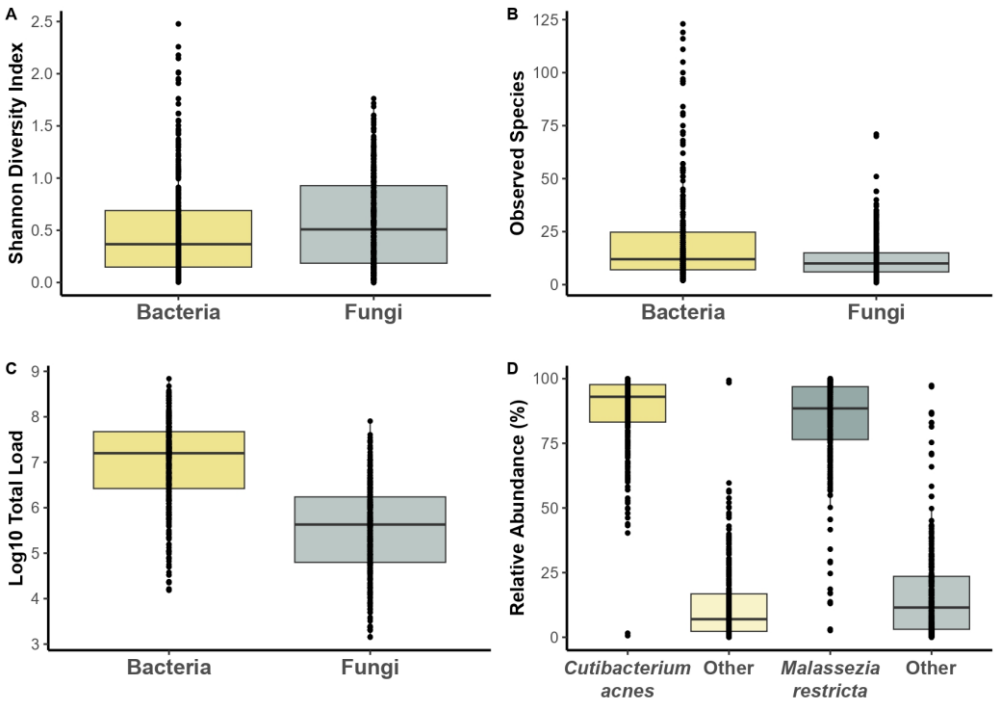

Figure 1. Microbiome composition and diversity metrics for Cluster 1. (**A**) Shannon diversity index, (**B**) Species richness, (**C**) Total bacterial and fungal load, (**D**) Relative abundance of dominant taxa.

Table 4. Cluster 1 demographic distribution of age, skin facial concerns, sensitivity, and skin type by skin conditions (Healthy, Inflamed, Other). Values in each skin condition column are in percentage. This table presents the demographic characteristics of 362 participants categorized into Healthy, Inflamed, and Other subgroups within Cluster 1 (n = 364).

Category	Subcategory/Item	Healthy (n = 86)	Inflamed (n = 242)	Other (n = 34)	Total (n = 362)
Age Range	8–18 (Puberty)	0.0	1.2	0.0	0.8
	19–30 (Early Reproductive)	17.4	24.8	14.7	22.1
	31–40 (Mid Reproductive)	41.9	50.8	50.0	48.6
	41–45 (Late Reproductive)	16.3	12.4	11.8	13.3
	46–55 (Perimenopause)	11.6	7.9	14.7	9.4
	>55 (Postmenopause)	12.8	2.9	8.8	5.8
Facial Skin Concerns	Acne/breakouts	0.0	39.5	15.7	31.1
	Wrinkles	45.6	21.3	18.6	24.7
	Hyperpigmentation	20.4	18.0	8.6	17.4
	Rosacea	0.0	12.9	4.3	10.1
	Eczema	0.0	7.2	2.9	5.7
	Psoriasis	0.0	1.2	1.4	1.0
	None	34.0	0.0	0.0	5.1
	Other	0.0	0.0	48.6	5.0
Skin Sensitivity	Yes	36.0	66.9	64.7	59.4
	No	64.0	33.1	35.3	40.6
Skin Type	Balanced	39.5	12.4	5.9	18.2
	Combination	27.9	53.3	44.1	46.4
	Dry	26.7	22.7	44.1	25.7
	Oily	4.7	10.3	2.9	8.3
	Unknown	1.2	1.2	2.9	1.4

Note: All data, except Age Range, were self-reported and self-evaluated by the participants.

3.2. Intra-Cluster Stratification of Healthy vs. Inflamed Subgroups

Alpha diversity analysis revealed that bacterial evenness (Figure 2A) and richness (Figure 2B) were significantly lower in the Inflamed group compared to the other two groups, while no significant differences in fungal alpha diversity were observed among the three groups (Figure 2E,F). This demonstrates that skin inflammation is associated with a reduction in bacterial diversity, while fungal diversity remains conserved across skin conditions.

Beta diversity analysis using Bray–Curtis dissimilarity and PERMANOVA indicated significant differences in overall microbial community structure for both bacteria (Figure 2C) and fungi (Figure 2G) across the groups. This illustrates that inflamed skin harbors unique bacterial and fungal communities relative to healthy skin. While fungal alpha diversity remains stable, community composition shifts significantly, parallel to the compositional changes observed in the bacterial community.

In the bacterial community, *Staphylococcus epidermidis* showed a decreasing trend in the Inflamed group compared to the Healthy group, while *C. acnes* exhibited a tendency toward higher abundance in the Inflamed group relative to both Healthy and Other groups. *Corynebacterium bovis* was not detected in the Other group (Figure 2D). In addition, *Corynebacterium pseudogenitalium* was significantly reduced in the Inflamed group compared to both the Healthy (adjusted p = 0.0001) and Other (adjusted p = 0.001) groups.

Among fungal taxa, *Cladosporium* was lower in abundance in both the Inflamed and Other groups compared to Healthy, while *Saccharomyces cerevisiae* was more abundant in the Inflamed (Figure 2H) and particularly in the Other group with skin sensitivity (Figure S1d), although the difference was not significant. *Malassezia globosa* was significantly less abundant in the Inflamed group compared to the Healthy group (adjusted $p = 0.045$).

When groups were further stratified by the presence or absence of self-reported skin sensitivity, the overall trend of reduced bacterial diversity in the Inflamed group was maintained. However, the difference was no longer statistically significant among individuals without sensitivity, while it remained significant in the sensitivity subgroup (Figure S1a). Interestingly, within the non-sensitive subgroup, the Other group exhibited significantly lower fungal diversity compared to both the Healthy and Inflamed groups (Figure S1c). Taxonomic analysis revealed that *Corynebacterium kroppenstedtii* was more abundant in the Healthy group with sensitivity, whereas this increase was not observed in the Inflamed or Other groups, regardless of sensitivity status (Figure S1b).

Together, our findings suggest a higher prevalence and diversity of *Corynebacterium* species within the healthy cohort compared to the inflamed group. Notably, the inflamed group also exhibited a higher percentage of self-reported skin sensitivity, a condition often associated with impaired barrier function. Based on these microbiome characteristics, we adopted two previously developed fermentation-derived cosmetic ingredients with reported skin-related biological activities [35–38] for the Cluster 1-oriented formulation. Ambioter, derived from culture filtrate of *Corynebacterium amycolatum* SB-1, was selected for its potential relevance to inflammation-associated skin concerns. Fillerstin, derived from culture filtrates of *Streptococcus pneumoniae, Streptococcus mitis*, and *Streptococcus infantis*, was selected for its potential relevance to collagen-related and skin barrier functions.

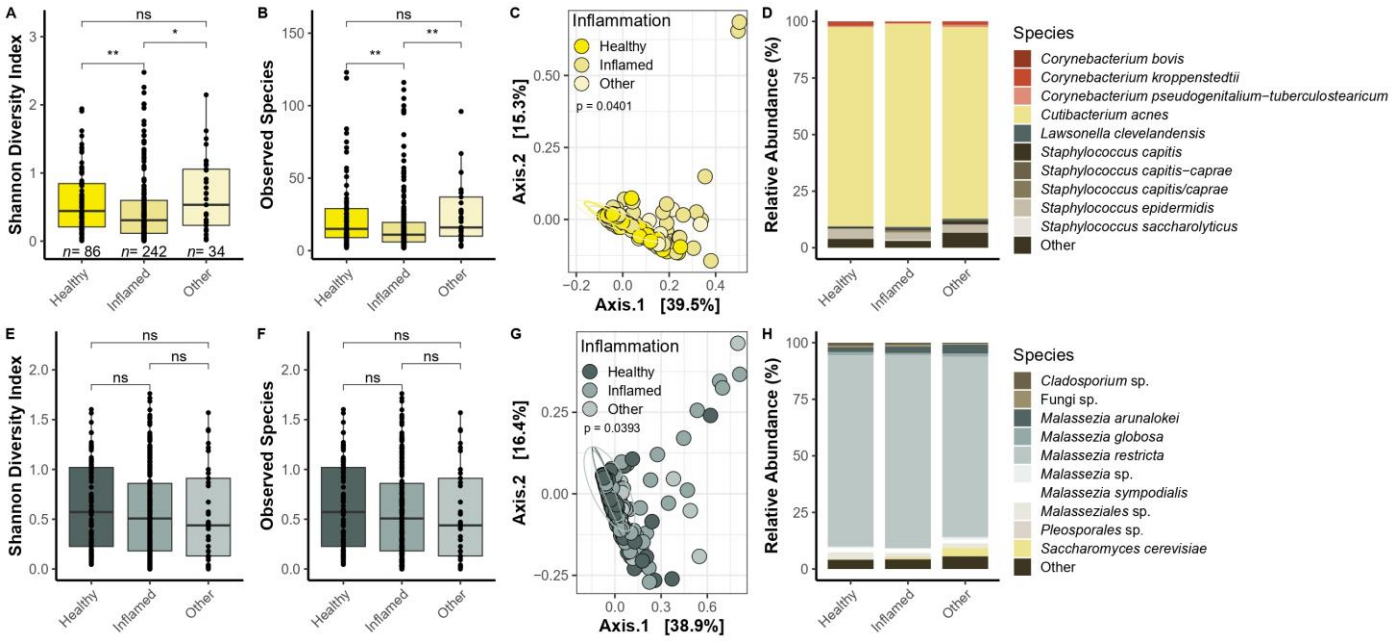

Figure 2. Microbiome composition of target Cluster 1. (**A**) Bacterial Shannon diversity, (**B**) bacterial species richness, (**C**) Bacterial community structure (Bray–Curtis dissimilarity PCoA), (**D**) bacterial relative abundance, (**E**) fungal Shannon diversity, (**F**) fungal species richness, (**G**) fungal community structure (Bray–Curtis dissimilarity PCoA), and (**H**) fungal relative abundance. * $p < 0.05$, ** $p < 0.01$. Adonis *p*-value indicates significance of group separation.

3.3. Ingredient Isolation and Efficacy Data for Postbiotic Ambioter and Fillerstin

We evaluated the effects of Fillerstin on key skin-related gene expression in UV-damaged human dermal fibroblasts. Treatment with 1% *Streptococcus* culture filtrate, the fermentation-derived component of Fillerstin, significantly upregulated the mRNA expression of *COL1A1*, a gene encoding for pro-alpha1 chains which is a key component of type I collagen, showing a 1.51-fold increase compared to the UV-treated control group ($p < 0.05$; Figure 3a). This finding suggests that the *Streptococcus* culture filtrate may partially restore *COL1A1* mRNA expression under UV-induced stress conditions, although the observed 1.51-fold increase represents a modest effect. In contrast, MMP-1 mRNA expression was significantly reduced to 0.54-fold that of UV-damaged cells following treatment with the *Streptococcus* culture filtrate ($p < 0.05$), suggesting a potential effect on collagen degradation-related gene expression.

We further evaluated the anti-inflammatory effects of Ambioter by analyzing the gene expression of *IL-1β*, a known pro-inflammatory factor, in cells treated with Poly (I:C) 10 μg/ml plus IL-4 10 ng/ml ($p < 0.05$; Figure 3b). Treatment with 1% Ambioter significantly reduced *IL-1β* gene expression from 1.87-fold to 1.38-fold relative to the control conditions.

To examine topical allergic reactions to the postbiotic ferments, HRIPT was performed, and skin irritation was assessed. Each ingredient passed HRIPT. Based on the test population of 51 subjects, and under the conditions of this study, the ingredient did not demonstrate a potential for eliciting dermal irritation or inducing sensitization. They also passed three toxicity tests. In an in vitro skin irritation test using the Reconstructed Human Epidermis model, each item was judged to be Non-Irritant (NI): UN GHS "No Category" in skin irritation. They did not show an indication of mutagenic potential under the conditions. In an in vitro eye irritation test using the Reconstructed human Cornea-like Epithelium (RhCE) model, each ingredient was judged to be Non-Irritant (NI): UN GHS "No Category".

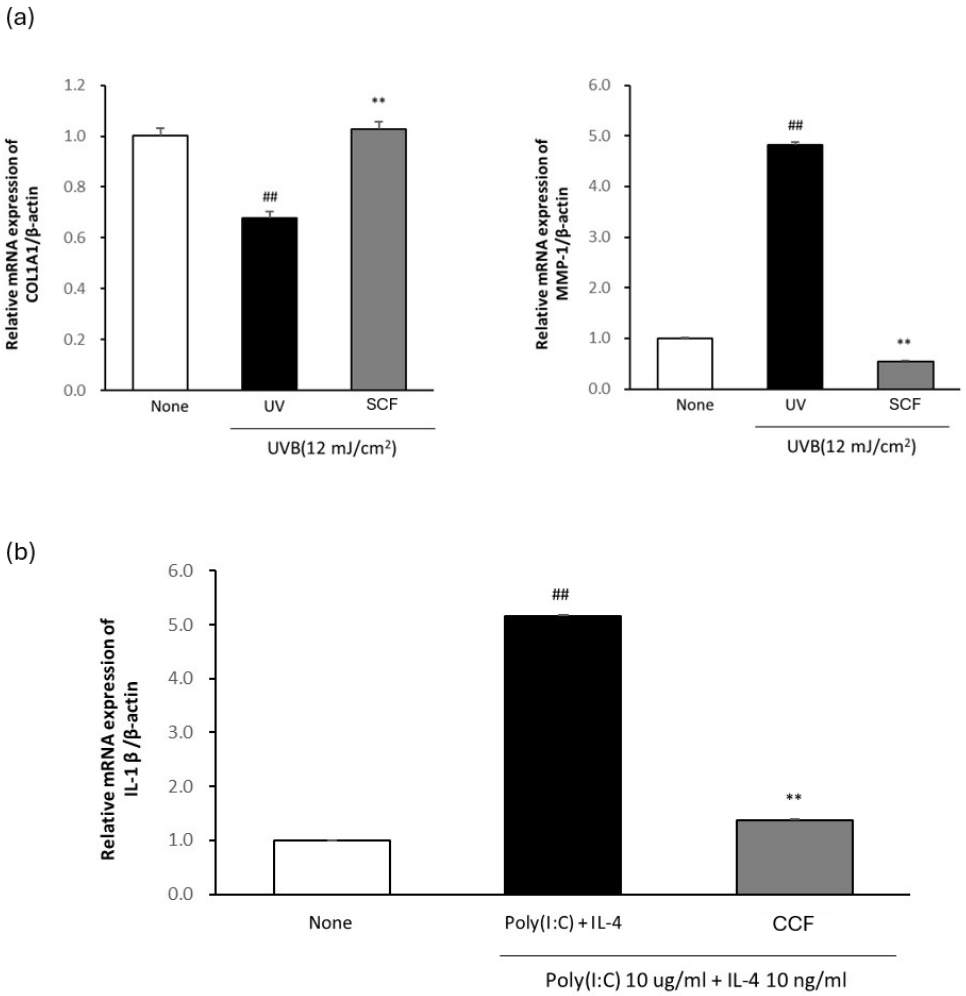

Figure 3. Effects of postbiotic ferments on gene expression related to collagen regulation and inflammation. (**a**) Expression levels of *COL1A1* and *MMP-1* in Hs68 cells treated with 1% (*w*/*w*) *Streptococcus* culture filtrate (SCF), the fermentation-derived component of Fillerstin. ## p <0.01 vs. None, ** p < 0.01 vs. UV. (**b**) Gene expression levels of IL-1β in HaCaT cells treated with 1% (*w*/*w*) *Corynebacterium* culture filtrate (CCF), the fermentation-derived component of Ambioter. ## p <0.01 vs. None, ** p < 0.01 vs. Inducer. Data are presented as mean ± SD from three independent biological experiments (n = 3).

3.4. Cluster 1-Specific Formulation Approach

Cluster 1 exhibits a fair to medium skin tone, with a predominance of combination to dry skin with sensitivity and a notable proportion of oily skin. This complex skin profile involves both sebum excess and barrier weakness, requiring a multi-faceted care approach. To address these needs, we developed targeted cleanser and serum formulations (Tables 2 and 3) incorporating the postbiotic complex Fillerstin, a cosmetic ingredient containing culture filtrate derived from *Streptococcus pneumoniae*, *Streptococcus mitis*, and *Streptococcus infantis*, along with preservative components. The corresponding *Streptococcus* culture filtrates were evaluated for their effects on collagen-related gene expression (Figure 3a). In addition, Ambioter, a cosmetic ingredient containing *Corynebacterium amycolatum* SB-1 culture filtrate and preservative components, was included alongside niacinamide and tetrahexyldecyl ascorbate (a vitamin C derivative) to target inflammation-associated skin concerns (Figure 3b). The commercial cosmetic ingredients Fillerstin and Ambioter were each incorporated at 1% (*w*/*w*) in both the cleanser and serum formulations, corresponding to ingredients No. 200 and 190 in Table

2 and No. 180 and 170 in Table 3, respectively. This ingredient strategy was designed to provide comprehensive care for Cluster 1 skin, addressing sensitivity, dryness, oiliness, and uneven tone simultaneously.

Both Fillerstin and Ambioter showed negative results in the bacterial reverse mutation assays, with and without metabolic activation. In the in vitro skin irritation tests, the mean tissue viabilities were 95.8% and 98.2% for Fillerstin and Ambioter, respectively, exceeding the non-irritant classification threshold of 50%. In the in vitro eye irritation tests, the corresponding mean tissue viabilities were 104.2% and 100.6%, respectively, exceeding the non-irritant classification threshold of 35%. Both ingredients were classified as non-irritants under the respective test conditions. In the ingredient-level HRIPTs, 51 participants completed the assessments. Both undiluted Fillerstin and Ambioter were classified as non-irritating, with skin irritation indices of 0.00. No skin reactions were recorded during the challenge phase, and no adverse events were reported.

The safety of the final facial serum was further evaluated using an HRIPT. A total of 119 participants were enrolled in the HRIPT, including 60 participants with self-perceived sensitive skin. Of these, 112 participants completed the study, including 56 with self-perceived sensitive skin (Table 5a). Under the conditions of this study, the test material identified as our facial serum did not demonstrate a potential for eliciting dermal irritation or inducing sensitization (Table 5b).

Table 5. HRIPT participant demographics including (**a**) self-perceived skin sensitivity, gender, age, and final sample size and (**b**) dermal response summary.

(**a**)

Number of Participants	Skin Type *		Sex		Age			Final Participants	
119	Sensitive Skin	Normal Skin	Female	Male	Minimum	Maximum	Mean (SD)	Number of Participants	Dropout (%)
	60	59	89	30	18	69	48.68 (14.50)	112	5.88

(**b**)

Subject	Induction Scores									Challenge Scores			
Number	1	2	3	4	5	6	7	8	9	24 h.	48 h.	72 h.	96 h.
6	0	0	0	0	0	0	DISCONTINUED						
12	0	0	0	DISCONTINUED									
22	0	DISCONTINUED											
28	0	0	0	DISCONTINUED									
31	0	0	0	0	0	0	0	0	0	0	0	X	0
43	0	0	0	0	0	0	0	0	0	0	0	0	---
53	0	0	0	0	0	0	0	0	0	0	0	0	X
57	0	0	0	0	0	0	0	0	0	0	0	X	0
87	0	0	0	0	0	0	0	0	0	0	X	X	DISC
88	0	0	0	0	0	0	0	0	0	DISCONTINUED			
90	0	0	0	0	0	0	0	0	0	X	0	0	X
92	0	0	0	0	0	0	0	0	0	0	0	0	X
97	0	0	0	0	0	0	0	0	0	0	0	0	X
103	0	0	0	0	0	0	0	0	0	0	0	0	X
108	0	0	0	0	0	0	0	0	0	0	0	0	X
114	0	0	0	0	0	0	0	0	0	0	0	X	0
116	0	0	DISCONTINUED										

* Sensitive skin: self-perceived sensitive skin. 0—No visible skin reaction; X = Subject absent; --- = No reading; DISC = Discontinued.

https://doi.org/10.3390/microorganisms14122742

3.5. Skin Microbiome Assessment During Use of the Skincare Regimen

To evaluate skin microbiome and clinical outcomes during use of the skincare regimen containing postbiotic ferments, we conducted a six-week clinical study in which 43 participants completed the study. One participant was excluded from the longitudinal microbiome analysis due to a missing baseline microbiome sample, resulting in a final analysis cohort of 42 participants. The facial cleanser was used for the first two weeks, followed by the combined use of the cleanser and serum for the subsequent four weeks. Amplicon sequencing was performed on 126 samples collected from forehead skin at baseline, Week 2, and Week 6. Table 1 summarizes the demographic and self-reported characteristics of the 42 participants included in the microbiome analysis, including ethnicity, skin characteristics, and hormonal factors stratified by age group.

To assess longitudinal changes in the skin microbiome during use of the regimen, we compared bacterial and fungal community profiles across three time points. No statistically significant changes in Shannon diversity indices were observed across the three time points for either bacterial or fungal communities (Figure 4A,D). Principal Coordinate Analysis (PCoA) based on Bray–Curtis dissimilarity revealed no statistically significant differences in overall community composition among the three time points for either bacteria or fungi (PERMANOVA, $p = 0.99$ and $R^2 = 0.0039$ for bacteria; $p = 0.70$ and $R^2 = 0.0119$ for fungi; Figure 4B,E). At the taxon level, none of the top ten most abundant bacterial taxa exhibited significant changes in relative abundance across time points (Figure 4C). Similarly, no statistically significant changes were observed among the top ten fungal taxa. However, a decreasing trend in the relative abundance of *M. globosa* and *M. restricta* was detected from Baseline to Week 6, although this trend did not reach statistical significance (Figure 4F).

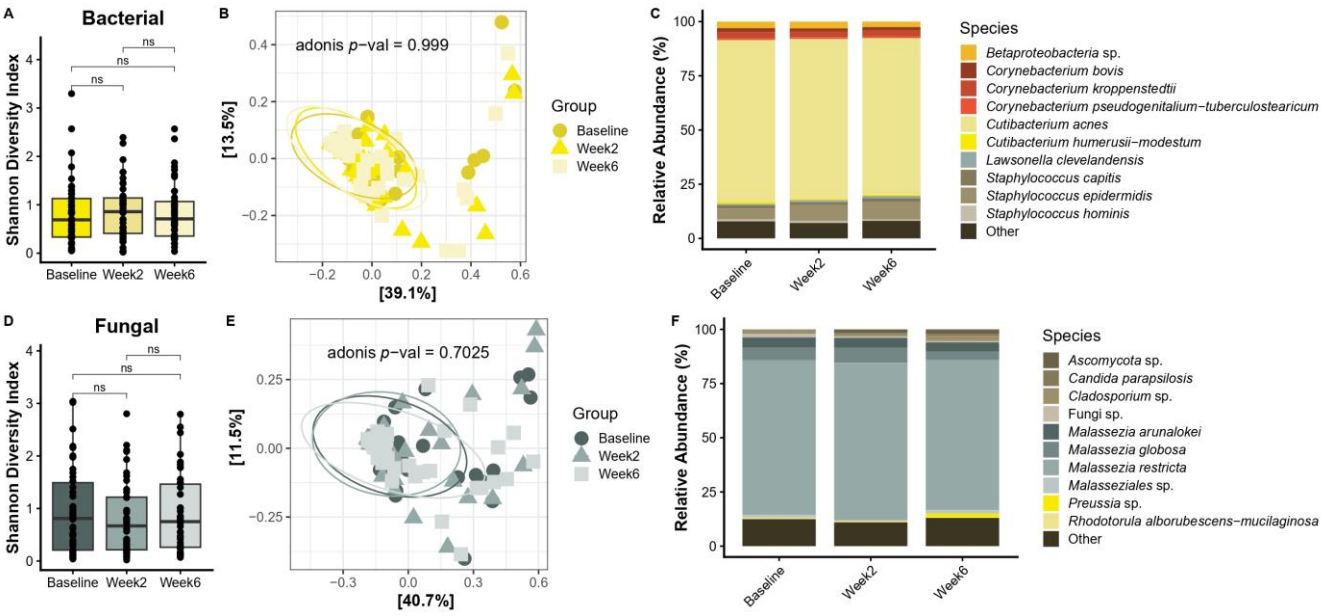

Figure 4. Temporal dynamics of microbiome composition post-treatment. (**A**) Bacterial Shannon diversity, (**B**) bacterial community structure (Bray–Curtis dissimilarity PCoA), (**C**) bacterial relative abundance, (**D**) fungal Shannon diversity, (**E**) fungal community structure (Bray–Curtis dissimilarity PCoA), and (**F**) fungal relative abundance. ADONIS *p*-value indicates significance of group separation.

3.6. Clinical Outcomes During Use of the Skincare Regimen

We evaluated changes in multiple skin parameters from baseline during use of the study regimen (Table 6). Several parameters showed improvements from baseline at Week 2 and/or Week 6.

Among the parameters assessed, luminosity/radiance and skin texture showed statistically significant improvements relative to baseline at Week 2 (both $p = 0.0313$). At Week 6, both parameters also showed significant improvements relative to baseline (both $p < 0.0001$). These observations indicate changes during the skincare regimen but do not establish a progressive treatment effect or effects attributable specifically to the postbiotic ingredients.

In contrast, fine lines/wrinkles, evenness of skin tone, dark circles, visibility of pores, sebum production, and elasticity (R6) showed numerical improvements at Week 2 that did not reach statistical significance. By Week 6, following use of the combined cleanser-and-serum regimen, all six parameters showed statistically significant improvements relative to baseline (Table 6). Notably, sebum production decreased by 24.4% relative to baseline ($p = 0.0086$). Other Cutometer-derived elasticity parameters showed no statistically significant changes relative to baseline (Table S2).

Hydration measurements followed a distinct pattern of change over time. At Week 2, hydration decreased numerically relative to baseline (−4.7%, $p = 0.2219$). At Week 6, hydration showed a statistically significant increase relative to baseline (+7.9%, $p = 0.0391$; Table 6). In contrast, transepidermal water loss (TEWL) was significantly lower at Week 2 than at baseline (−7.5%, $p = 0.0034$), but did not differ significantly from baseline at Week 6 ($p = 0.8927$; Table 6). These findings should be interpreted cautiously given the uncontrolled study design and the sequential introduction of the serum.

Table 6. Post-treatment changes in skin physical parameters. Decreased values indicate improvement for expert clinical grading, sebumeter (sebum production), cutometer R6 ratio (elasticity), and vapometer (transepidermal water loss). Increase corneometer values indicate improved hydration levels. NA: significance testing not applicable.

Method/Category	Parameters	Baseline	Week 2	Week 6	Week 2 vs. Baseline	Week 6 vs. Baseline
Expert Clinical Grading	Finelines and Wrinkles (Visual)	2.02	2.02	1.86	NA	−7.9% ($p = 0.0156$)
	Evenness of Skin Tone (Visual)	3.88	3.81	3.49	−1.8% ($p = 0.2500$)	−10.1% ($p < 0.0001$)
	Skin Texture (Visual)	4.07	3.93	3.44	−3.4% ($p = 0.0313$)	−15.5% ($p < 0.0001$)
	Luminosity/Radiance	4.21	4.07	3.37	−3.3% ($p = 0.0313$)	−20.0% ($p < 0.0001$)
	Vasc. Dark Circles (Visual)	2.09	2.02	1.79	−3.3% ($p = 0.2500$)	−14.4% ($p = 0.0020$)
	Visibility of Pores	3.77	3.67	3.49	−2.7% ($p = 0.1250$)	−7.4% ($p = 0.0010$)
Sebumeter	Sebum Production	88.8	80.1	67.1	−9.8% ($p = 0.2078$)	−24.4% ($p = 0.0086$)
Cutometer	Elasticity (R6)	0.6293	0.5828	0.5440	−7.4% ($p = 0.1556$)	−13.6% ($p = 0.0056$)
Corneometer	Hydration	57.2	54.5	61.7	−4.7% ($p = 0.2219$)	+7.9% ($p = 0.0391$)
Vapometer	Trans-epidermal water loss	12.0	11.1	12.1	−7.5% ($p = 0.0034$)	+0.83% ($p = 0.8927$)

Clinical assessments were performed in 43 participants at baseline, Week 2, and Week 6. Statistical comparisons were conducted using the Wilcoxon signed-rank test for expert clinical grading,

paired-sample *t*-tests for Sebumeter, Cutometer, and VapoMeter measurements, and a paired-sample t-test (Week 2) or Wilcoxon signed-rank test (Week 6) for Corneometer measurements. Reported *p*-values were not adjusted for multiple comparisons and should be interpreted as exploratory.

3.7. Linking Microbiome Signatures to Clinical Outcomes

To explore potential associations between the skin microbiome and physical parameters, we performed Spearman's rank correlation analyses between dominant microbial taxa and individual parameters. Notably, both *C. kroppenstedtii* and *M. globosa* abundances significantly correlate with worsening skin evenness, luminosity, and texture (Figure 5A,B). Though *C. kroppenstedtii* significantly associated with poor skin conditions at baseline and Week 2, this association became non-significant by Week 6 (Figure S2a-c). Further, while *M. globosa* correlated with poorer skin conditions (skin evenness, luminosity, and texture) at Week 2, this relationship attenuated by Week 6, showing both reduced correlation strength and loss of statistical significance (Figure S3a-c). These exploratory associations changed over time during use of the regimen; they do not establish that the regimen altered the taxa or their clinical impact. Both species also displayed a decreasing trend with regimen usage, though neither reached statistical significance. In addition to these shared patterns, *C. kroppenstedtii* showed a significant correlation with worsening fine lines (Figure 5A, Figure S2d), while *M. globosa* abundance was significantly negatively correlated with hydration levels (Figure 5B, Figure S3d).

C. acnes abundance was significantly correlated with improved fine lines (Figure 5A and Figure S4a), and the bacterial class *Betaproteobacteria* was significantly correlated with worsening dark circles (Figure 5A and Figure S4b).

Among non-Malassezia fungal taxa, the phylum *Ascomycota* showed a significant negative correlation with sebum production at both Week 2 and 6 (Figure 5B and Figure S5a), suggesting an association between its relative abundance and sebum levels. Meanwhile, *Curvularia* sp. abundance was significantly associated with clinical severity in skin evenness and fine lines (Figure 5B and Figure S5b,c).

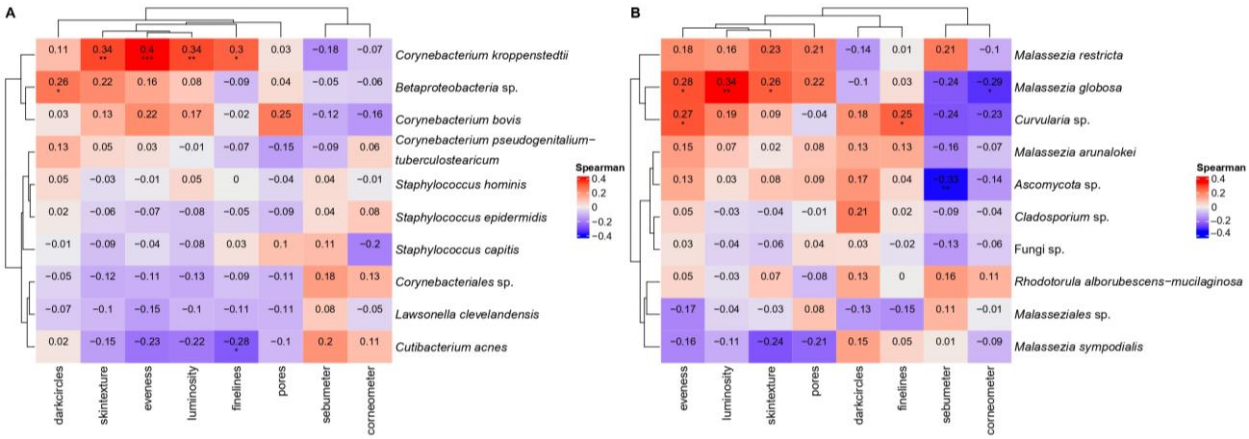

Figure 5. Spearman's rank correlations between skin parameters and dominant microbial taxa. (**A**) Top 10 bacterial taxa. (**B**) Top 10 fungal taxa. Color scale indicates correlation coefficient (blue: negative correlation; red: positive correlation). Skin parameters include expert clinical grading (vascular dark circles, skin texture, evenness of skin tone, luminosity/radiance, fine lines/wrinkles, and pores visibility) and instrumental measurements (Sebumeter, Corneometer). Adjusted *p*-values using Benjamini–Hochberg method for multiple comparisons are indicated by * $p < 0.05$, ** $p < 0.01$, *** $p < 0.001$.

4. Discussion

In this study, we employed an unsupervised machine learning approach to identify eight distinct skin microbiome clusters based on facial microbiome profiles, focusing on the largest cluster (Cluster 1) for targeted formulation development. Cluster 1 represents younger individuals and was dominated by *C. acnes* and *M. restricta*, with low microbial diversity and high prevalence of self-reported skin sensitivity, oily, or combination skin. Thus, we focused on microbiome-informed skincare strategies tailored to inflammation- and acne-prone skin types.

We developed a targeted serum formulation incorporating postbiotic actives Fillerstin and Ambioter alongside niacinamide and tetrahexyldecyl ascorbate (a vitamin C derivative). In vitro experiments showed that the *Streptococcus* culture filtrate, the fermentation-derived component of Fillerstin, increased *COL1A1* mRNA expression and decreased *MMP-1* mRNA expression in UV-exposed fibroblasts. Similarly, the *Corynebacterium* culture filtrate, the fermentation-derived component of Ambioter, reduced *IL-1β* mRNA expression in an inflammatory cell model. These findings suggest potential collagen-related and anti-inflammatory activities under the tested in vitro conditions. Importantly, both postbiotic ingredients underwent HRIPT and in vitro toxicity assessments, with no evidence of irritation or sensitization under the tested conditions. During the clinical study, use of the complete regimen was associated with improvements in selected skin parameters, while no statistically significant changes in alpha diversity or overall microbial community composition were detected over the study period. Additionally, certain microbial taxa showed correlations with clinical parameters, suggesting their potential as candidate biomarkers of skin health status. Several limitations should be considered when interpreting the clinical findings. First, the study employed a single-arm design without a vehicle or comparator control, limiting causal attribution of the observed skin improvements. Second, the serum contained multiple active ingredients, including Fillerstin, Ambioter, niacinamide, and tetrahexyldecyl ascorbate. Therefore, the individual contributions of these components could not be distinguished. Furthermore, participants used the cleanser alone during the first two weeks and both the cleanser and serum during the subsequent four weeks, making it difficult to separate the effects of treatment duration from those associated with the introduction of the serum. Accordingly, the observed clinical changes should be interpreted as changes associated with the overall skincare regimen rather than evidence of postbiotic-specific efficacy. Future randomized, vehicle-controlled studies are needed to determine the independent contributions of the postbiotic ingredients.

Interestingly, a subset of individuals within the same cluster, despite sharing similar microbial dominance patterns, presented with non-inflamed, healthy skin. This intra-cluster breakdown between healthy and inflamed subgroups identifies subtle microbial and host-associated differences, enabling more precise characterization of skin dysbiosis drivers. Further stratification revealed that reductions in *S. epidermidis* and *Corynebacterium species*, particularly *C. pseudogenitalium*, along with a non-significant increase in the commensal yet opportunistic *C. acnes*, were associated with inflamed and sensitive skin states. *C. pseudogenitalium* abundance was significantly lower in inflamed skin compared to healthy skin in our study. Experimental studies have highlighted the roles of selected non-diphtherial *Corynebacterium* species in cutaneous immune modulation and interbacterial interactions in a species- and context-dependent manner [49,50]. *S. epidermidis* has been widely recognized for its beneficial effects on the skin, including the production of antimicrobial peptides, modulation of immune tolerance, and reinforcement of skin barrier integrity [51–53]. These findings suggest a potential association of *C. pseudogenitalium* with skin condition and support the established role of *S. epidermidis* in skin health and barrier function.

https://doi.org/10.3390/microorganisms14122742

In contrast, *C. acnes* plays a dual role in skin health. As a dominant commensal organism, it contributes to lipid metabolism, acidic pH maintenance, and pathogen defense through short-chain fatty acids production (e.g., propionic acid), which inhibits pathogens and supports barrier integrity [54,55]. However, certain *C. acnes* strains have been implicated in inflammatory skin conditions such as acne vulgaris, particularly through activation of innate immune responses, biofilm formation, and stimulation of pro-inflammatory cytokines [26,56]. Thus, the role of *C. acnes* is highly strain-dependent (phylotype-dependent), with clades such as IA1 and IA2 more commonly associated with inflammatory acne lesions, whereas types IB and II are often found in healthy skin [57,58].

Furthermore, the correlations between microbial relative abundances and skin parameters should be considered exploratory, given the compositional nature of microbiome data and the multiple comparisons performed in a relatively small cohort. These associations do not establish causal relationships between individual microbial taxa and clinical outcomes.

The absence of statistically significant changes in microbial alpha or beta diversity during the study does not establish microbiome stability or explain the mechanisms underlying the observed clinical changes. This observation is consistent with previous reports suggesting that improvements in skin barrier function and clinical outcomes may occur without substantial changes in microbial community structure [59,60]. However, further studies are needed to determine whether the skincare regimen preserves microbiome homeostasis or induces functional microbial changes that are not captured by diversity analyses.

The observed correlations between specific microbial species and skin parameters provide insights into potential host–microbe interactions in skin health. Positive correlations between *C. kroppenstedtii* and *M. globosa* relative abundances and less favorable skin texture, evenness, and luminosity scores suggest that these taxa may serve as potential microbial markers associated with skin condition. In Cluster 1, we observed that *C. kroppenstedtii* was more abundant in healthy individuals who self-reported sensitive skin compared to those without sensitivity, even within the healthy cohort. These findings are consistent with prior studies that have shown an increase in *C. kroppenstedtii* with age and skin sensitivity [29,30,61]. A recent study has found that *M. globosa* exacerbates skin inflammation by stimulating human keratinocyte IL-23 secretion and subsequently inducing pathogenic Th17 cell differentiation [62]. Notably, these correlations appeared weaker following the combined use of the cleanser and serum, although this observation does not establish a causal effect of the skincare regimen on the relationships between microbial taxa and skin parameters. These species-specific relationships highlight the importance of examining individual taxa rather than solely focusing on community-level metrics.

The discovery cohort used for clustering was a self-selected, direct-to-consumer convenience sample assembled without demographic or eligibility filtering; its representativeness of any defined population therefore cannot be judged, and the cluster prevalences and associated "skin segment" descriptions should be interpreted as exploratory rather than population-level estimates. Participants in the clinical study were selected using phenotypic criteria derived from Cluster 1 profile rather than by microbiome-based cluster assignment. Phenotypic matching is therefore not a direct measurement of cluster membership, and we cannot exclude the possibility that some participants would have been assigned to another cluster based on sequencing assessment. Confirmation of cluster membership is a priority for future work. We did not perform strain-level resolution of *C. acnes* populations, which represents a limitation. Without distinguishing between commensal and potentially pathogenic lineages, it remains unclear whether the observed increase in *C. acnes* abundance among the sensitive

and inflamed subgroups reflects a dysbiotic expansion of inflammatory strains or merely an overgrowth of benign commensals. Future studies employing shotgun metagenomics or single locus sequence typing (SLST) will be essential to clarify these distinctions and further elucidate the precise role of *C. acnes* in skin dysbiosis and health. Additionally, the postbiotic serum may induce functional shifts in the microbiome, such as altered metabolite production, without affecting taxonomic composition, a possibility that warrants future metagenomic or metabolomic approaches.

Although previous studies and ingredient-level HRIPTs provide supporting evidence of biological activity and dermal tolerability, cell viability was not directly assessed under the specific concentrations and exposure conditions used in the present in vitro experiments. In addition, the in vitro experiments were conducted at a single concentration (1% *w*/*w*), and the observed changes were assessed at the mRNA level without protein-level validation. The use of a single reference gene (*β-actin*) also represents a methodological limitation, and future studies should include dose–response analyses, protein-level measurements, and validation using multiple reference genes. Therefore, the possibility that changes in cell viability contributed to the observed gene-expression responses cannot be fully excluded. Future studies should include direct cell viability assessments to confirm that the observed effects are independent of cytotoxicity. Furthermore, the clinical study included only female participants aged 20–45 years, which limits the generalizability of the findings to other age groups and sexes. Participant attrition should also be considered when interpreting the observed clinical changes.

5. Conclusions

This study provides preliminary evidence supporting the feasibility of microbiome-informed skincare formulation development based on microbial and physiological skin characteristics. During the six-week skincare regimen, improvements in several skin parameters were observed relative to baseline, while no statistically significant changes in microbial alpha or beta diversity were detected. However, the uncontrolled study design and the inclusion of multiple active ingredients prevent attribution of the observed clinical improvements, specifically to the postbiotic ingredients. These findings provide a foundation for further investigation of microbiome-informed skincare approaches, and future randomized, controlled studies are needed to establish their clinical efficacy, validate the personalization approach, and determine the specific contributions of postbiotic ingredients.

Supplementary Materials: The following supporting information can be downloaded at: https://www.mdpi.com/article/10.3390/microorganisms14122742/s1. Table S1: Primer sequences used for microbiome profiling and gene expression analysis. Table S2: Improvements in cutometer measurements post-treatment. Decreased R0 indicates improved firmness. Increased R2, R5, and R7 ratios indicate improved elasticity. Table S3: Sizes of the eight skin microbiome clusters identified by unsupervised k-means clustering. Figure S1: Microbiome composition stratified by skin sensitivity in target cluster. (a) Bacterial Shannon diversity (b) Bacterial relative abundance (c) Fungal Shannon diversity (d) Fungal relative abundance $*p < 0.05$, $**p < 0.01$. Figure S2: Time-series of Spearman's rank correlation between skin physical parameters and *Corynebacterium kroppenstedtii* including (a) skin texture measurements (b) skin evenness (c) luminosity (d) fine lines. Figure S3: Time-series of Spearman's rank correlation between skin physical parameters and *Malassezia globosa* including (a) skin evenness (b) luminosity (c) skin texture (d) corneometer. Figure S4: Time-series of Spearman's rank correlation between (a) *Cutibacterium acnes* and fine lines (b) *Betaproteobacteria* sp and dark circles. Figure S5: Time-series of Spearman's rank correlation between (a) *Ascomycota* sp and sebum levels, *Curvularia* sp and (b) skin evenness and (c) fine lines.

Author Contributions: H.-B.K. and U.T.N. contributed equally to this manuscript**.** Conceptualization, S.K. and H.G.P.; Formal Analysis, U.T.N. and H.-B.K.; Investigation, H.-B.K.; Data Curation, M.Y., N.L., E.J., H.J., M.K. (Minji Kim)., M.K. (Misun Kim), D.-G.L., C.H.P., Y.N., S.L. and J.J.; Writing—Original Draft Preparation, U.T.N.; Writing—Review & Editing, H.-B.K., M.Y., N.L., E.J., H.J., M.K. (Minji Kim), M.K. (Misun Kim), D.-G.L., C.H.P., Y.N., S.L. and J.J.; Visualization, U.T.N.; Supervision, S.K. and H.G.P. and D.K.Y.; Project Administration, S.K. and H.G.P. All authors have read and agreed to the published version of the manuscript.

Funding: This research was funded by COSMAX Inc.

Institutional Review Board Statement: The study was conducted in accordance with the Declaration of Helsinki, and the protocol was approved by the Ethic Committee of Advarra (Columbia, Maryland, USA) (IRB Protocol Number: ECRLNJ2025-0446 BI) on 18 June 2025 for the collection of human skin microbiome samples with pre- and post-regimen images. The collection of human facial skin samples in this study was approved by the Ethics Committee of the H&BIO Corporation R&D CENTER (H&BIO, South Korea) (IRB Protocol Number: HBABN01-210217-HR-0181-01) on 7 February 2021.

Informed Consent Statement: Written informed consent was obtained from all participants involved in the study.

Data Availability Statement: The de-identified data supporting the findings of this study are available from the corresponding author upon reasonable request, subject to applicable privacy and ethical restrictions.

Conflicts of Interest: H.-B.K., H.J., Minji Kim, Misun Kim, D.-G.L., and C.H.P. were employed by COSMAX BTI. U.T.N., M.Y., N.L., E.J., and H.G.P. were employed by HelloBiome (ELSI Skin Health Inc.). Y.N., S.L., and J.J. were employed by COSMAX USA. S.K. was employed by COSMAX. COSMAX BTI funded the study, which involved fermentation-derived cosmetic ingredients developed for commercial applications. D.K.Y. declares no conflicts of interest. COSMAX Co., Ltd. holds intellectual property related to the *Streptococcus* and *Corynebacterium* strains and their skin-related applications described in this study (KR20240118638A and KR102321536B1).

References

1. Byrd, A.L.; Belkaid, Y.; Segre, J.A. The Human Skin Microbiome. *Nat. Rev. Microbiol.* **2018**, *16*, 143–155. https://doi.org/10.1038/nrmicro.2017.157.
2. Grice, E.A.; Segre, J.A. The Skin Microbiome. *Nat. Rev. Microbiol.* **2011**, *9*, 244–253. https://doi.org/10.1038/nrmicro2537.
3. Schommer, N.N.; Gallo, R.L. Structure and Function of the Human Skin Microbiome. *Trends Microbiol.* **2013**, *21*, 660–668. https://doi.org/10.1016/j.tim.2013.10.001.
4. Gallo, R.L. Human Skin Is the Largest Epithelial Surface for Interaction with Microbes. *J. Investig. Dermatol.* **2017**, *137*, 1213–1214. https://doi.org/10.1016/j.jid.2016.11.045.
5. Costello, E.K.; Lauber, C.L.; Hamady, M.; Fierer, N.; Gordon, J.I.; Knight, R. Bacterial Community Variation in Human Body Habitats Across Space and Time. *Science* **2009**, *326*, 1694–1697. https://doi.org/10.1126/science.1177486.
6. Grice, E.A.; Kong, H.H.; Conlan, S.; Deming, C.B.; Davis, J.; Young, A.C.; Bouffard, G.G.; Blakesley, R.W.; Murray, P.R.; Green, E.D.; et al. Topographical and Temporal Diversity of the Human Skin Microbiome. *Science* **2009**, *324*, 1190–1192. https://doi.org/10.1126/science.1171700.
7. Oh, J.; Byrd, A.L.; Park, M.; Kong, H.H.; Segre, J.A. Temporal Stability of the Human Skin Microbiome. *Cell* **2016**, *165*, 854–866. https://doi.org/10.1016/j.cell.2016.04.008.
8. Salem, I.; Ramser, A.; Isham, N.; Ghannoum, M.A. The Gut Microbiome as a Major Regulator of the Gut-Skin Axis. *Front. Microbiol.* **2018**, *9*, 1459. https://doi.org/10.3389/fmicb.2018.01459.
9. Sanford, J.A.; Gallo, R.L. Functions of the Skin Microbiota in Health and Disease. *Semin. Immunol.* **2013**, *25*, 370–377. https://doi.org/10.1016/j.smim.2013.09.005.

10. Claesen, J.; Spagnolo, J.B.; Ramos, S.F.; Kurita, K.L.; Byrd, A.L.; Aksenov, A.A.; Melnik, A.V.; Wong, W.R.; Wang, S.; Hernandez, R.D.; et al. A *Cutibacterium acnes* Antibiotic Modulates Human Skin Microbiota Composition in Hair Follicles. *Sci. Transl. Med.* **2020**, *12*, eaay5445. https://doi.org/10.1126/scitranslmed.aay5445.
11. Zipperer, A.; Konnerth, M.C.; Laux, C.; Berscheid, A.; Janek, D.; Weidenmaier, C.; Burian, M.; Schilling, N.A.; Slavetinsky, C.; Marschal, M.; et al. Human Commensals Producing a Novel Antibiotic Impair Pathogen Colonization. *Nature* **2016**, *535*, 511–516. https://doi.org/10.1038/nature18634. Erratum in *Nature* **2016**, *539*, 314.
12. Alam, S.A.; Mandal, S.M. Guardians of the Epidermis: Interplay Between Skin Microbiota and Antimicrobial Peptides. In *Evolution of Antimicrobial Peptides*; Springer Nature: Cham, Switzerland, 2024; pp. 81–101.
13. Belkaid, Y.; Segre, J.A. Dialogue between Skin Microbiota and Immunity. *Science* **2014**, *346*, 954–959. https://doi.org/10.1126/science.1260144.
14. Sanford, J.A.; Zhang, L.-J.; Williams, M.R.; Gangoiti, J.A.; Huang, C.-M.; Gallo, R.L. Inhibition of HDAC8 and HDAC9 by Microbial Short-Chain Fatty Acids Breaks Immune Tolerance of the Epidermis to TLR Ligands. *Sci. Immunol.* **2016**, *1*, eaah4609. https://doi.org/10.1126/sciimmunol.aah4609.
15. Sanford, J.A.; O'Neill, A.M.; Zouboulis, C.C.; Gallo, R.L. Short-Chain Fatty Acids from *Cutibacterium acnes* Activate Both a Canonical and Epigenetic Inflammatory Response in Human Sebocytes. *J. Immunol.* **2019**, *202*, 1767–1776. https://doi.org/10.4049/jimmunol.1800893.
16. Harris-Tryon, T.A.; Grice, E.A. Microbiota and Maintenance of Skin Barrier Function. *Science* **2022**, *376*, 940–945. https://doi.org/10.1126/science.abo0693.
17. Wang, Z.; Mascarenhas, N.; Eckmann, L.; Miyamoto, Y.; Sun, X.; Kawakami, T.; Di Nardo, A. Skin Microbiome Promotes Mast Cell Maturation by Triggering Stem Cell Factor Production in Keratinocytes. *J. Allergy Clin. Immunol.* **2017**, *139*, 1205–1216.e6. https://doi.org/10.1016/j.jaci.2016.09.019.
18. Grice, E.A. The Intersection of Microbiome and Host at the Skin Interface: Genomic- and Metagenomic-Based Insights. *Genome Res.* **2015**, *25*, 1514–1520. https://doi.org/10.1101/gr.191320.115.
19. Oh, J.; Byrd, A.L.; Deming, C.; Conlan, S.; Kong, H.H.; Segre, J.A. Biogeography and Individuality Shape Function in the Human Skin Metagenome. *Nature* **2014**, *514*, 59–64. https://doi.org/10.1038/nature13786.
20. Scharschmidt, T.C.; Fischbach, M.A. What Lives on Our Skin: Ecology, Genomics and Therapeutic Opportunities of the Skin Microbiome. *Drug Discov. Today Dis. Mech.* **2013**, *10*, e83–e89. https://doi.org/10.1016/j.ddmec.2012.12.003.
21. Gardner, S.E.; Hillis, S.L.; Heilmann, K.; Segre, J.A.; Grice, E.A. The Neuropathic Diabetic Foot Ulcer Microbiome Is Associated with Clinical Factors. *Diabetes* **2013**, *62*, 923–930. https://doi.org/10.2337/db12-0771.
22. Kalan, L.; Loesche, M.; Hodkinson, B.P.; Heilmann, K.; Ruthel, G.; Gardner, S.E.; Grice, E.A. Redefining the Chronic-Wound Microbiome: Fungal Communities Are Prevalent, Dynamic, and Associated with Delayed Healing. *mBio* **2016**, *7*, e01058-16. https://doi.org/10.1128/mBio.01058-16.
23. Kalan, L.R.; Meisel, J.S.; Loesche, M.A.; Horwinski, J.; Soaita, I.; Chen, X.; Uberoi, A.; Gardner, S.E.; Grice, E.A. Strain- and Species-Level Variation in the Microbiome of Diabetic Wounds Is Associated with Clinical Outcomes and Therapeutic Efficacy. *Cell Host Microbe* **2019**, *25*, 641–655.e5. https://doi.org/10.1016/j.chom.2019.03.006.
24. Kong, H.H.; Oh, J.; Deming, C.; Conlan, S.; Grice, E.A.; Beatson, M.A.; Nomicos, E.; Polley, E.C.; Komarow, H.D.; Murray, P.R.; et al. Temporal Shifts in the Skin Microbiome Associated with Disease Flares and Treatment in Children with Atopic Dermatitis. *Genome Res.* **2012**, *22*, 850–859. https://doi.org/10.1101/gr.131029.111.
25. Tett, A.; Pasolli, E.; Farina, S.; Truong, D.T.; Asnicar, F.; Zolfo, M.; Beghini, F.; Armanini, F.; Jousson, O.; De Sanctis, V.; et al. Unexplored Diversity and Strain-Level Structure of the Skin Microbiome Associated with Psoriasis. *npj Biofilms Microbiomes* **2017**, *3*, 14. https://doi.org/10.1038/s41522-017-0022-5.
26. Barnard, E.; Shi, B.; Kang, D.; Craft, N.; Li, H. The Balance of Metagenomic Elements Shapes the Skin Microbiome in Acne and Health. *Sci. Rep.* **2016**, *6*, 39491. https://doi.org/10.1038/srep39491. Erratum in *Sci. Rep.* **2020**, *10*, 6037.
27. Cavallo, I.; Sivori, F.; Truglio, M.; De Maio, F.; Lucantoni, F.; Cardinali, G.; Pontone, M.; Bernardi, T.; Sanguinetti, M.; Capitanio, B.; et al. Skin Dysbiosis and *Cutibacterium acnes* Biofilm in Inflammatory Acne Lesions of Adolescents. *Sci. Rep.* **2022**, *12*, 21104. https://doi.org/10.1038/s41598-022-25436-3.
28. Han, J.H.; Kim, H.S. Skin Deep: The Potential of Microbiome Cosmetics. *J. Microbiol.* **2024**, *62*, 181–199. https://doi.org/10.1007/s12275-024-00128-x.
29. Zhou, W.; Fleming, E.; Legendre, G.; Roux, L.; Latreille, J.; Gendronneau, G.; Forestier, S.; Oh, J. Skin Microbiome Attributes Associate with Biophysical Skin Ageing. *Exp. Dermatol.* **2023**, *32*, 1546–1556. https://doi.org/10.1111/exd.14863.

30. Park, H.G.; Swaney, M.H.; Nguyen, U.T.; Lukianets, N.; Jungman, E. Redefining the Skin Type: Microbiome-Based Segmentation for Efficient Product Development and Personalization. *IFSCC Mag.* **2023**, *26*, 295–301.
31. Park, H.G.; Cheung, S.; Lukianets, N.; Jungman, E. How the Fungal Mycobiome Uncovers Insights on Skin Health and Aging. Available online: https://www.cosmeticsandtoiletries.com/research/methods-tools/article/22892426/cosmetics-toiletries-magazine-how-fungal-data-extends-microbiome-insights-on-skin-health-and-aging (accessed on 13 November 2026).
32. Gueniche, A.; Perin, O.; Bouslimani, A.; Landemaine, L.; Misra, N.; Cupferman, S.; Aguilar, L.; Clavaud, C.; Chopra, T.; Khodr, A. Advances in Microbiome-Derived Solutions and Methodologies Are Founding a New Era in Skin Health and Care. *Pathogens* **2022**, *11*, 121. https://doi.org/10.3390/pathogens11020121.
33. Sun, C.; Hu, G.; Yi, L.; Ge, W.; Yang, Q.; Yang, X.; He, Y.; Liu, Z.; Chen, W.-H. Integrated Analysis of Facial Microbiome and Skin Physio-Optical Properties Unveils Cutotype-Dependent Aging Effects. *Microbiome* **2024**, *12*, 163. https://doi.org/10.1186/s40168-024-01891-0.
34. Cogen, A.L.; Nizet, V.; Gallo, R.L. Skin Microbiota: A Source of Disease or Defence? *Br. J. Dermatol.* **2008**, *158*, 442–455. https://doi.org/10.1111/j.1365-2133.2008.08437.x.
35. Kim, G.; Kim, M.; Kim, M.; Park, C.; Yoon, Y.; Lim, D.-H.; Yeo, H.; Kang, S.; Lee, Y.-G.; Beak, N.-I.; et al. Spermidine-Induced Recovery of Human Dermal Structure and Barrier Function by Skin Microbiome. *Commun. Biol.* **2021**, *4*, 231. https://doi.org/10.1038/s42003-020-01619-4.
36. Kim, M.S.; Kim, H.J.; Kang, S.M.; Heo, Y.M.; Kang, J.; Ryu, T.K.; Kim, H.J.; Choi, Y.; Kim, S.; Nho, Y.H.; et al. Efficacy and Safety of Topical Streptococcus Postbiotic Emollient in Adolescents and Adults with Mild-to-moderate Atopic Dermatitis: A Randomized, Double-blind, Vehicle-controlled Trial. *Allergy* **2024**, *79*, 1612–1616. https://doi.org/10.1111/all.16077.
37. Kang, J.; Yim, Y.; Lee, H.; Kang, S.M.; Lee, D.-G.; Heo, Y.M.; Jo, H.; Kang, S.; Kim, H.J.; Yon, D.K.; et al. Subtype-Specific Efficacy of Topical Streptococcus Postbiotic Emollient in Adolescents and Adults with Atopic Dermatitis and Comorbid Allergies: A Post-Hoc Analysis of a Randomized, Double-Blind, Vehicle-Controlled Trial. *Allergy Asthma Immunol. Res.* **2026**, *18*, 611–619. https://doi.org/10.4168/aair.2026.18.4.611.
38. Kim, S.; Mun, S.; Kim, M.; Kim, M.-J.; Lee, D.-G.; Kang, S.; Jo, H.; Han, K. Skin-Related Effects of *Corynebacterium amycolatum* SB-1 Ferment Filtrate and Functional Characterization of Ellagic Acid. *bioRxiv* **2026**, https://doi.org/10.64898/2026.09.02.748710.
39. Callahan, B.J.; McMurdie, P.J.; Rosen, M.J.; Han, A.W.; Johnson, A.J.A.; Holmes, S.P. DADA2: High-Resolution Sample Inference from Illumina Amplicon Data. *Nat. Methods* **2016**, *13*, 581–583. https://doi.org/10.1038/nmeth.3869.
40. Burton, M.; Krumbeck, J.A.; Wu, G.; Tang, S.; Prem, A.; Gupta, A.K.; Dawson, T.L. The Adult Microbiome of Healthy and Otitis Patients: Definition of the Core Healthy and Diseased Ear Microbiomes. *PLoS ONE* **2022**, *17*, e0262806. https://doi.org/10.1371/journal.pone.0262806.
41. Edgar, R.C. Search and Clustering Orders of Magnitude Faster than BLAST. *Bioinformatics* **2010**, *26*, 2460–2461. https://doi.org/10.1093/bioinformatics/btq461.
42. DeSantis, T.Z.; Hugenholtz, P.; Larsen, N.; Rojas, M.; Brodie, E.L.; Keller, K.; Huber, T.; Dalevi, D.; Hu, P.; Andersen, G.L. Greengenes, a Chimera-Checked 16S rRNA Gene Database and Workbench Compatible with ARB. *Appl. Environ. Microbiol.* **2006**, *72*, 5069–5072. https://doi.org/10.1128/AEM.03006-05.
43. Abarenkov, K.; Nilsson, R.H.; Larsson, K.-H.; Alexander, I.J.; Eberhardt, U.; Erland, S.; Høiland, K.; Kjøller, R.; Larsson, E.; Pennanen, T.; et al. The UNITE Database for Molecular Identification of Fungi—Recent Updates and Future Perspectives. *New Phytol.* **2010**, *186*, 281–285. https://doi.org/10.1111/j.1469-8137.2009.03160.x.
44. Tang, S.; Prem, A.; Tjokrosurjo, J.; Sary, M.; Van Bel, M.A.; Rodrigues-Hoffmann, A.; Kavanagh, M.; Wu, G.; Van Eden, M.E.; Krumbeck, J.A. The Canine Skin and Ear Microbiome: A Comprehensive Survey of Pathogens Implicated in Canine Skin and Ear Infections Using a Novel next-Generation-Sequencing-Based Assay. *Vet. Microbiol.* **2020**, *247*, 108764. https://doi.org/10.1016/j.vetmic.2020.108764.
45. McMurdie, P.J.; Holmes, S. Phyloseq: An R Package for Reproducible Interactive Analysis and Graphics of Microbiome Census Data. *PLoS ONE* **2013**, *8*, e61217. https://doi.org/10.1371/journal.pone.0061217.
46. Heo, Y.M.; Lee, D.-G.; Mun, S.; Kim, M.; Baek, C.; Lee, H.; Yun, S.K.; Kang, S.; Han, K. Skin Benefits of Postbiotics Derived from *Micrococcus luteus* Derived from Human Skin: An Untapped Potential for Dermatological Health. *Genes Genom.* **2024**, *46*, 13–25. https://doi.org/10.1007/s13258-023-01471-w.
47. Kim, H.-B.; Kim, G.; Park, E.; Kim, H.; Yu, B.S.; Lee, D.-G.; Park, C.H.; Jo, H.; Park, H. Functional Expansion of the Skin Microbiome: A Pantothenate-Producing *Rothia* Strain Confers Anti-Inflammatory and Photoaging-Protective Effects. *Int. J. Mol. Sci.* **2025**, *26*, 12058. https://doi.org/10.3390/ijms262412058.

48. Park, Y.; Yu, B.S.; Heo, Y.M.; Kyung, S.; Lee, K.-E.; Kim, S.; Kang, S.; Han, K.; Kim, D.H. Characteristics of *Malassezia furfur* at Various pH and Effects of *Malassezia* Lipids on Skin Cells. *Appl. Microbiol. Biotechnol.* **2024**, *108*, 455. https://doi.org/10.1007/s00253-024-13292-2.
49. Ridaura, V.K.; Bouladoux, N.; Claesen, J.; Chen, Y.E.; Byrd, A.L.; Constantinides, M.G.; Merrill, E.D.; Tamoutounour, S.; Fischbach, M.A.; Belkaid, Y. Contextual Control of Skin Immunity and Inflammation by *Corynebacterium*. *J. Exp. Med.* **2018**, *215*, 785–799. https://doi.org/10.1084/jem.20171079.
50. Ramsey, M.M.; Freire, M.O.; Gabrilska, R.A.; Rumbaugh, K.P.; Lemon, K.P. *Staphylococcus aureus* Shifts toward Commensalism in Response to *Corynebacterium* Species. *Front. Microbiol.* **2016**, *7*, 1230. https://doi.org/10.3389/fmicb.2016.01230.
51. Cogen, A.L.; Yamasaki, K.; Muto, J.; Sanchez, K.M.; Crotty Alexander, L.; Tanios, J.; Lai, Y.; Kim, J.E.; Nizet, V.; Gallo, R.L. *Staphylococcus epidermidis* Antimicrobial δ-Toxin (Phenol-Soluble Modulin-γ) Cooperates with Host Antimicrobial Peptides to Kill Group A *Streptococcus*. *PLoS ONE* **2010**, *5*, e8557. https://doi.org/10.1371/journal.pone.0008557.
52. Nakatsuji, T.; Chen, T.H.; Butcher, A.M.; Trzoss, L.L.; Nam, S.-J.; Shirakawa, K.T.; Zhou, W.; Oh, J.; Otto, M.; Fenical, W.; et al. A Commensal Strain of *Staphylococcus epidermidis* Protects against Skin Neoplasia. *Sci. Adv.* **2018**, *4*, eaao4502. https://doi.org/10.1126/sciadv.aao4502.
53. Zheng, Y.; Hunt, R.L.; Villaruz, A.E.; Fisher, E.L.; Liu, R.; Liu, Q.; Cheung, G.Y.C.; Li, M.; Otto, M. Commensal *Staphylococcus epidermidis* Contributes to Skin Barrier Homeostasis by Generating Protective Ceramides. *Cell Host Microbe* **2022**, *30*, 301–313.e9. https://doi.org/10.1016/j.chom.2022.01.004.
54. Almoughrabie, S.; Cau, L.; Cavagnero, K.; O'Neill, A.M.; Li, F.; Roso-Mares, A.; Mainzer, C.; Closs, B.; Kolar, M.J.; Williams, K.J.; et al. *Commensal Cutibacterium acnes* Induce Epidermal Lipid Synthesis Important for Skin Barrier Function. *Sci. Adv.* **2023**, *9*, eadg6262. https://doi.org/10.1126/sciadv.adg6262.
55. Park, H.; Arellano, K.; Lee, Y.; Yeo, S.; Ji, Y.; Ko, J.; Holzapfel, W. Pilot Study on the Forehead Skin Microbiome and Short Chain Fatty Acids Depending on the SC Functional Index in Korean Cohorts. *Microorganisms* **2021**, *9*, 2216. https://doi.org/10.3390/microorganisms9112216.
56. Cha, J.; Kim, T.-G.; Ryu, J.-H. Conversation between Skin Microbiota and the Host: From Early Life to Adulthood. *Exp. Mol. Med.* **2025**, *57*, 703–713. https://doi.org/10.1038/s12276-025-01427-y.
57. Fitz-Gibbon, S.; Tomida, S.; Chiu, B.-H.; Nguyen, L.; Du, C.; Liu, M.; Elashoff, D.; Erfe, M.C.; Loncaric, A.; Kim, J.; et al. *Propionibacterium acnes* Strain Populations in the Human Skin Microbiome Associated with Acne. *J. Investig. Dermatol.* **2013**, *133*, 2152–2160. https://doi.org/10.1038/jid.2013.21.
58. Yu, Y.; Champer, J.; Agak, G.W.; Kao, S.; Modlin, R.L.; Kim, J. Different *Propionibacterium acnes* Phylotypes Induce Distinct Immune Responses and Express Unique Surface and Secreted Proteomes. *J. Investig. Dermatol.* **2016**, *136*, 2221–2228. https://doi.org/10.1016/j.jid.2016.06.615.
59. Wang, D.-Q.; Li, X.; Zhang, R.-Y.; Yuan, C.; Yan, B.; Humbert, P.; Quan, Z.-X. Effects of Investigational Moisturizers on the Skin Barrier and Microbiome Following Exposure to Environmental Aggressors: A Randomized Clinical Trial and Ex Vivo Analysis. *J. Clin. Med.* **2023**, *12*, 6078. https://doi.org/10.3390/jcm12186078.
60. Lebeer, S.; Oerlemans, E.F.M.; Claes, I.; Henkens, T.; Delanghe, L.; Wuyts, S.; Spacova, I.; van den Broek, M.F.L.; Tuyaerts, I.; Wittouck, S.; et al. Selective Targeting of Skin Pathobionts and Inflammation with Topically Applied Lactobacilli. *Cell Rep. Med.* **2022**, *3*, 100521. https://doi.org/10.1016/j.xcrm.2022.100521.
61. Filaire, E.; Vialleix, C.; Cadoret, J.-P.; Guénard, S.; Muller, C.; Dreux-Zigha, A.; Berthon, J.-Y. Characterization of Reactive and Sensitive Skin Microbiota: Effect of Halymenia Durvillei (HD) Extract Treatment. *Cosmetics* **2019**, *6*, 69. https://doi.org/10.3390/cosmetics6040069.
62. Jia, Q.; Hu, J.; Wang, X.; Deng, Y.; Zhang, J.; Li, H. *Malassezia globosa* Induces Differentiation of Pathogenic Th17 Cells by Inducing IL-23 Secretion by Keratinocytes. *Mycopathologia* **2024**, *189*, 85. https://doi.org/10.1007/s11046-024-00890-x.

Disclaimer/Publisher's Note: The statements, opinions and data contained in all publications are solely those of the individual author(s) and contributor(s) and not of MDPI and/or the editor(s). MDPI and/or the editor(s) disclaim responsibility for any injury to people or property resulting from any ideas, methods, instructions or products referred to in the content.